МОЛОДОЙ УЧЁНЫЙ

CXXII Международная научная конференция

ИССЛЕДОВАНИЯ МОЛОДЫХ УЧЕНЫХ

КАЗАНЬ

Часть 1

УДК 005(063)
ББК 65.290-2я43
И88

И88 **Исследования молодых ученых** : материалы CXXII Междунар. науч. конф. (г. Казань, апрель 2026 г.) / [под ред. И. Г. Ахметова и др.]. — Казань : Молодой ученый, 2026. — iv, 140 с.

ISBN 978-5-6054100-7-2.

В сборнике представлены материалы CXXII Международной научной конференции «Исследования молодых ученых».

Предназначен для научных работников, преподавателей, аспирантов и студентов, а также для широкого круга читателей.

УДК 005(063)
ББК 65.290-2я43

ISBN 978-5-6054100-7-2

СОДЕРЖАНИЕ

ИНФОРМАТИКА

АРХИТЕКТУРА И СТРОИТЕЛЬСТВО

ТЕХНИЧЕСКИЕ НАУКИ

МЕДИЦИНА И ФАРМАКОЛОГИЯ

СЕЛЬСКОЕ ХОЗЯЙСТВО

МЕНЕДЖМЕНТ

ИНФОРМАТИКА

City-scale threat trajectory aggregation across heterogeneous camera networks: a conceptual deep learning framework

Adda-Abbu Ahmed-Reda, master's degree student
Moscow Polytechnic University

Deep learning architectures for single-camera video analysis have reached a high level of maturity in clip-level action recognition and anomaly detection, yet the transition to city-scale threat detection — spanning thousands of heterogeneous, uncalibrated cameras including fixed CCTV, pan-tilt-zoom units, and aerial drones — remains an open and largely unaddressed problem. Real threats in urban environments manifest as multi-site trajectories unfolding over minutes to hours, crossing administrative boundaries and network segments that no single inference node can observe in full. This paper formulates city-scale, calibration-free threat trajectory aggregation as an unsolved problem in urban AI surveillance and proposes a conceptual hierarchical framework to address it. The architecture extends prior single-site work by introducing four novel components: a federated edge-inference layer that distributes per-camera processing across geographically separated nodes; a dynamic topology graph that replaces the static camera adjacency maps of single-site systems with a live, event-aware city graph; a cross-modal fusion stage that integrates video streams with auxiliary urban sensors — audio arrays, license plate readers, and access-control logs — without requiring metric calibration between modalities; and a cross-jurisdiction propagation mechanism that enables threat context to traverse administrative domain boundaries without exchanging raw video data. The anomaly scoring model from prior work is preserved and extended with a fourth component, network-level anomaly, which captures coordinated multi-actor threats invisible to per-person scoring. Three illustrative urban scenarios demonstrate the conceptual reach of the framework. The paper is architectural in nature; experimental validation is identified as the primary direction for future work.

Keywords: *city-scale surveillance, federated inference, dynamic topology graph, cross-modal fusion, threat trajectory, multi-camera Re-ID, deep learning, urban security.*

1. Introduction

A city is not a shopping mall scaled up. A mall has dozens of cameras, a single operator room, a known floor plan, and a bounded perimeter. A city has hundreds of thousands of cameras belonging to different agencies, operated by different software stacks, with no shared clock, no shared coordinate system, and no shared identity of the people moving through it. The threat that unfolds across a mall in minutes may unfold across a city in hours.

Prior work on multi-camera threat detection [15] addressed the single-site problem: how to aggregate threat signals across a bounded, topologically static network of uncalibrated cameras. That framework produced a hierarchical pipeline combining SlowFast [1] for local action recognition, VideoMAE v2 [3] for view-invariant re-identification embeddings, and a graph-transformer for trajectory-level anomaly scoring decomposed into three components: local, spatial, and temporal. The architecture was conceptually sound for its scope. But city-scale surveillance breaks every assumption that made the single-site problem tractable.

Four assumptions fail in particular. First, topology is no longer static: a camera network covering a city changes continuously as mobile units — drones, vehicle-mounted cameras, PTZ units with shifting fields of view — enter and leave the observable space. Second, processing cannot be centralised: the bandwidth required to pipe raw video from thousands of cameras to a single inference server is physically infeasible at urban scale, necessitating a distributed, federated architecture. Third, video is no longer the only modality: urban security infrastructure routinely includes acoustic sensors, license plate recognition systems, access-control logs, and cellular positioning data, all of which carry independent threat signals that a video-only architecture cannot exploit. Fourth, and distinctly, cameras do not belong to a single administrative domain: in practice, urban surveillance infrastructure spans municipal police networks, transit authorities, private operators, and federal installations, each governed by different data-sharing regulations that legally prohibit raw video from crossing jurisdictional boundaries. This fourth failure mode — administrative fragmentation — is not a technical limitation but a legal and organisational one, yet it is equally capable of rendering a city-scale architecture inoperable if unaddressed.

This paper makes four contributions. First, it formulates city-scale calibration-free threat trajectory aggregation as a distinct and unsolved problem, explicitly identifying the four failure modes above as the gap between single-site capabilities and urban-scale requirements. Second, it proposes a federated hierarchical framework that addresses each failure mode with a dedicated architectural component: a distributed edge-inference layer, a dynamic topology graph, a cross-modal fusion stage, and a cross-jurisdiction propagation mechanism. Third, it extends the anomaly decomposition of prior work [15] with a fourth component — network-level anomaly — that captures coordinated multi-actor threats whose individual trajectories may each appear innocuous. Fourth, it strengthens the theoretical basis of the network-level anomaly component by distinguishing coordinated threat movement from coincidental convergence in dense urban environments.

The paper is organised as follows. Section 2 reviews the relevant architectural building blocks and their limitations at city scale. Section 3 formalises the problem. Section 4 describes the proposed framework. Section 5 illustrates it on three urban threat scenarios. Section 6 discusses limitations and open questions.

2. Architectural Building Blocks: Capabilities and City-Scale Limits

The core video understanding components carry over from prior single-site work [15] with the same capabilities and the same fundamental limitation: all operate on short clips from a single camera and produce no inter-node representations. SlowFast R50 [1] achieves 77.0% top-1 on Kinetics-400 and remains the practical choice for real-time per-camera action recognition. Video Swin-B [2] reaches 84.9% and is preferable in dense scenes requiring precise interaction localisation. VideoMAE v2 ViT-g [3] achieves 90.0% top-1 and produces view-invariant embeddings by virtue of self-supervised pre-training on masked reconstruction — the property exploited for calibration-free re-identification.

At city scale, four additional components become load-bearing. Federated learning frameworks such as FedAvg [16] demonstrate that model aggregation across geographically distributed nodes can maintain accuracy close to centralised training while eliminating the need to transmit raw data. This property is essential for urban surveillance, where data sovereignty constraints may prevent raw video from leaving the network segment of its originating agency. Federated inference — applying a trained model at edge nodes and transmitting only compressed representations to a central aggregator — is the operational counterpart to federated training.

Dynamic graph neural networks [17] extend static graph transformers to settings where node and edge sets evolve over time. In the urban surveillance context, nodes represent active camera feeds and mobile sensor units; edges represent observed or estimated transition probabilities between coverage zones. The ability to add and remove nodes without retraining the entire aggregation model is a prerequisite for integrating drone feeds and PTZ units whose coverage zones shift continuously.

Cross-modal fusion has been studied extensively in audio-visual settings [18], but the specific problem of fusing heterogeneous urban sensor streams — video, acoustic, license plate, access-control — without metric calibration between modalities has received little attention. The absence of a shared coordinate system means that traditional sensor fusion methods requiring explicit spatial alignment are inapplicable; instead, temporal co-occurrence and semantic compatibility must serve as the alignment signal.

Cross-jurisdiction data propagation is a component with no direct precedent in single-site or multi-camera surveillance literature. The requirement is to propagate threat-relevant embeddings across administrative domain boundaries without transmitting personally identifiable raw data. Federated identity propagation — transmitting anonymised appearance embeddings rather than video — is the mechanism proposed here, and it requires explicit design at both the technical and governance levels. Table 1 summarises the capabilities of the main components with respect to the city-scale threat detection task/

Table 1. **Architectural components and their city-scale threat detection capabilities. Dashes indicate components not evaluated on standard benchmarks as standalone models**

Architecture	Temporal Horizon	Top-1 K-400	Re-ID Robustness	Multi-Camera Aggregation
SlowFast R50 [1]	Seconds	77.0%	Low	No
Video Swin-B [2]	Seconds — minutes	84.9%	Medium	No
VideoMAE v2 ViT-g [3]	Up to tens of seconds	90.0%	High (by design)	No
Federated Node (proposed)	Minutes — hours	—	High (via VideoMAE)	Yes, per node
Proposed Full Architecture	Minutes — hours	—	High	Yes, city-scale

3. Problem Formalisation

3.1. Scope and Definitions

Let an urban surveillance network consist of N sensor nodes S_1, S_2,..., SN, where each node is either a fixed camera, a PTZ unit, an aerial drone, or an auxiliary non-video sensor. Nodes are heterogeneous: they differ in resolution, frame rate, field of view, and modality. No two nodes share a common calibration; temporal synchronisation is approximate, with clock drift on the order of seconds between nodes belonging to different administrative domains.

Each video node produces a stream of person tracks, and each track is encoded by a local inference node into a compact multi-modal embedding: a concatenation of the action embedding from SlowFast and the appearance embedding from VideoMAE v2, as in prior work [15]. Non-video nodes produce timestamped event records — acoustic detections, license plate reads, door-entry logs — which are independently embedded by modality-specific encoders.

The central problem is: given the stream of embeddings and event records from all N nodes, construct cross-node person trajectories spanning time horizons of one minute to several hours, and assign to each trajectory an anomaly score sufficient to distinguish pre-attack surveillance, coordinated infiltration, and organised criminal activity from the normal movement patterns of an urban population.

3.2. Extended Anomaly Decomposition

Prior work [15] decomposed trajectory anomaly into three components: local anomaly Alocal (unusual actions in individual clips), spatial anomaly Aspatial (atypical routing between zones), and temporal anomaly Atemporal (unusual dwell times and trajectory durations). This decomposition is preserved and extended with a fourth component.

Network-level anomaly Anetwork captures the statistical unusualness of the relationships between multiple trajectories observed simultaneously. The key design challenge is distinguishing coordinated movement — which constitutes a genuine threat signal — from coincidental convergence, which is a routine feature of dense urban environments. In a busy transit hub at rush hour, for example, hundreds of independent trajectories will converge on the same platform within a narrow time window without any coordination whatsoever. A naive implementation of Anetwork would flag such events continuously, rendering it operationally useless.

The resolution of this challenge lies in the joint distribution of spatial origin diversity and temporal synchronisation. Coincidental convergence in dense environments typically involves trajectories originating from a small number of adjacent source zones — commuters from nearby platforms, shoppers from nearby entrances — because normal crowd flow is directionally structured. Coordinated multi-actor threats, by contrast, tend to exhibit a statistically distinctive pattern: high spatial diversity of origin points combined with anomalously tight temporal synchronisation. Five individuals arriving at a restricted zone from five different districts within a four-minute window is not the signature of coincidental convergence; it is the signature of a planned rendezvous. Anetwork is therefore computed as a function of two sub-components: origin-diversity score Dorigin, which measures the geographic spread of trajectory source zones over a configurable lookback window, and synchronisation score Ssync, which measures the tightness of the time distribution of arrivals relative to the expected distribution under independent random-walk behaviour. Formally:

$$A\_network = f(D\_origin, S\_sync, C\_cluster)$$

where Ccluster is a cluster coherence term that penalises trajectory sets whose pairwise appearance embeddings are too similar — a signal of pre-planned uniform appearance — and f is a learned combination function. This formulation suppresses false positives in high-density environments while remaining sensitive to coordinated threats whose signatures emerge precisely from the combination of spatial diversity and temporal precision that coincidental convergence does not produce.

The extended anomaly score over the full trajectory set Π is:

$$A(\Pi) = w_1 \cdot A\_local + w_2 \cdot A\_spatial + w_3 \cdot A\_temporal + w_4 \cdot A\_network, \Sigma w_i = 1$$

Weights are scenario-dependent: in a high-density public event, A_network may dominate; in a restricted-access facility, A_spatial will carry the greater share.

4. Conceptual Architecture

4.1. Overview

The proposed framework is a five-level hierarchy. Levels 1 and 2 replicate the detection, tracking, and local representation components of the single-site architecture [15] and run independently at each edge node. Levels 3 through 5 are new and address the four failure modes identified in Section 1: distributed aggregation (Level 3), dynamic topology management (Level 4), and cross-modal fusion with city-level threat scoring including cross-jurisdiction propagation (Level 5).

4.2. Level 1 — Distributed Detection and Tracking

Each video node runs YOLOv8 [10] and ByteTrack [11] locally, producing per-camera person tracks as in prior work. The critical constraint at city scale is that no raw video leaves the edge node: only track bounding boxes and their timestamps are forwarded to the Level 2 encoder. This constraint satisfies both the bandwidth limitations of urban networks and the data minimisation requirements of privacy regulation, and is a prerequisite for compliance with the administrative boundary constraints discussed in Section 1.

4.3. Level 2 — Federated Local Representation

At each edge node, SlowFast R50 and a lightweight VideoMAE v2 variant (ViT-B for computational feasibility) encode each active track into an action embedding and an appearance embedding respectively. These are concatenated into a local track embedding, which is the unit of data transmitted to the central aggregator. Transmission volume scales with the number of active tracks rather than with video resolution or frame rate, making the approach bandwidth-feasible even at large node counts.

The reconstruction error of VideoMAE v2, used in prior work as a local anomaly signal, is computed locally and transmitted as a scalar alongside the embedding. This preserves the interpretability of the local anomaly component without transmitting the full reconstruction.

Federated model updates allow edge nodes to contribute to improving the shared encoder without sharing raw video. Following the FedAvg protocol [16], each node periodically transmits model weight gradients to the central server, which aggregates them and returns an updated model. This is particularly important for handling the distribution shift between different urban zones — commercial districts, transit hubs, residential areas — each of which has a distinct normal behaviour distribution.

4.4. Level 3 — Calibration-Free Cross-Node Identity Matching

Cross-node identity matching follows the soft-assignment principle of prior work [15]: for each pair of tracks from different nodes, a match probability is computed as a function of embedding similarity and temporal feasibility. At city scale, the temporal feasibility constraint is replaced by a travel-time distribution derived from historical transition data between coverage zones — a function of both geographic distance and time of day, since urban travel times vary significantly with congestion.

A critical extension at city scale is the integration of auxiliary modality signals into the matching decision. A license plate read at a parking structure node and a person detection at the adjacent building entrance, co-occurring within a feasible time window, constitute corroborating evidence for a shared identity even if their video embeddings are not directly comparable. The cross-modal fusion mechanism described in Level 5 feeds back into identity matching at this level, creating a bidirectional dependency between the two.

4.5. Level 4 — Dynamic Topology Graph

The static topology graph of single-site surveillance — a fixed adjacency matrix representing typical transitions between camera zones — is insufficient at city scale for two reasons. First, mobile nodes such as drones and PTZ units continuously change their coverage zones, altering the graph structure in real time. Second, scheduled events — public gatherings, transportation disruptions, large-scale operations — predictably alter normal transition patterns, making historical statistics temporarily invalid.

The dynamic topology graph maintains two layers. The physical layer encodes geographic proximity and known connectivity between node coverage zones; this layer changes only when infrastructure changes. The statistical layer encodes current transition probabilities estimated from a rolling window of recent observations; this layer updates continuously and is weighted to down-weight historical data during detected anomalous periods, preventing the spatial anomaly component from being calibrated against already-anomalous baselines.

Dynamic graph neural networks [17] operating over this two-layer structure can propagate threat signals spatially: a detection at one node raises the anomaly prior for adjacent nodes, enabling the system to anticipate trajectory continuations rather than merely react to them.

4.6. Level 5 — Cross-Modal Fusion, Cross-Jurisdiction Propagation, and City-Level Threat Scoring

The top level of the framework aggregates all signals — video track embeddings from Level 2, identity match probabilities from Level 3, graph-propagated anomaly priors from Level 4, and event records from auxiliary sensors — into a unified threat assessment. It additionally manages the propagation of threat context across administrative domain boundaries.

Cross-modal alignment without metric calibration is achieved through temporal and semantic co-occurrence. Two events from different modalities are treated as potentially co-referential if they occur within a configurable time window and are associated with the same coverage zone. A transformer-based fusion encoder [18] takes the concatenated modality-specific embeddings of co-referential events and produces a joint representation. This architecture is preferred over simple late fusion — which treats modality outputs as independent inputs to a final classifier — because it allows inter-modal attention: the transformer can learn that an acoustic detection and a video detection at the same location are mutually reinforcing evidence, rather than treating them as additively independent. It is also preferred over attention bottlenecks [18] in their strict form because the absence of metric calibration between modalities means bottleneck dimensionality cannot be set by a principled alignment criterion; the full cross-attention formulation is more robust to this uncertainty. The attention mechanism naturally weights modalities by their informativeness: in a low-visibility environment, acoustic embeddings will receive higher attention weights than video embeddings of comparable or lower quality.

The network-level anomaly component Anetwork is computed at this level over the full set of active trajectory graphs. A graph-transformer with global attention tokens — following the Longformer architecture [12] applied to graph inputs — computes pairwise trajectory correlations and scores joint movement patterns against the baseline described in Section 3.2. The computational complexity of full pairwise attention is managed by restricting cross-trajectory attention to trajectories sharing at least one coverage zone within the recent time window.

Cross-jurisdiction threat propagation operates as follows. When a trajectory in administrative domain A receives an elevated anomaly score, the corresponding VideoMAE v2 appearance embedding — not the underlying video — is transmitted to the central aggregator with a threat-level tag. When a track in domain B subsequently produces an embedding that exceeds the match threshold against the stored threat embedding, the prior anomaly score from domain A is incorporated into the ongoing trajectory score in domain B. No raw video crosses the administrative boundary at any point. The mechanism is the technical implementation of the fourth architectural component identified in Section 1, and its privacy-preserving properties are a design requirement rather than an incidental feature.

The final output is the extended anomaly score A (Π) computed per trajectory and per trajectory cluster, with dominant component attribution enabling interpretable operator alerts. The city-level dashboard presents active high-anomaly trajectories on a map overlay of the dynamic topology graph, with colour coding by dominant anomaly type.

5. Illustrative Urban Scenarios

Note: the following scenarios are conceptual illustrations of the expected behaviour of the proposed framework, not results of experiments or simulations. Their purpose is to demonstrate which anomaly components would be activated in each case and why single-site analysis would be insufficient.

5.1. Scenario 1: Pre-Attack Urban Reconnaissance

An individual visits a transit hub three times over two hours, each time spending several minutes observing staff positions and access points before departing. Between visits, the same individual is detected by a license plate reader at a nearby parking structure and briefly appears on a drone feed covering the street approach. No single camera observes more than a three-minute fragment of this activity.

The temporal anomaly component accumulates across the three visits: the total dwell time in the hub far exceeds the statistical norm for the zone. The spatial anomaly component activates when the trajectory reconstructed from the three video fragments and the license plate record forms a circular pattern around the hub — a route type associated with low probability in the statistical topology layer. The cross-modal fusion at Level 5 increases the identity match confidence for the three video fragments by using the license plate read as a temporal anchor, despite the absence of direct camera-to-camera handoffs. Anetwork remains near baseline in this scenario since only a single actor is involved; the elevated composite score is driven primarily by Atemporal and Aspatial.

5.2. Scenario 2: Coordinated Multi-Actor Infiltration

Five individuals enter a government district through five different access points over a thirty-minute window. Each individual's trajectory is individually unremarkable: the spatial routes are all within normal parameters, and no action recognition system flags unusual behaviour. After forty minutes, all five are detected within a single restricted zone.

Individual anomaly scores remain below alert threshold throughout. The network-level anomaly component is the decisive signal here. The five trajectories exhibit high spatial origin diversity — five different district entry points — combined with a tight arrival time distribution at the restricted zone that falls well below the expected variance under independent random-walk behaviour. The Dorigin sub-component scores high because no normal crowd dynamic produces simultaneous convergence from five geographically separated origins onto a single low-traffic node. The Ssync sub-component scores high because the arrival times cluster within four minutes despite origin distances that would, under normal transit patterns, produce a much wider spread. This joint pattern is the signature of coordinated movement, not coincidental convergence. The dynamic topology graph propagates elevated anomaly priors to the restricted zone from the moment the fourth individual's trajectory is linked to the emerging cluster pattern, enabling a pre-convergence alert rather than a post-incident detection.

5.3. Scenario 3: Cross-Jurisdiction Threat Trajectory

A person of interest is observed in an aggressive confrontation on a camera belonging to municipal authority A. The individual then moves into a district covered by cameras belonging to municipal authority B, where no prior context is available. Standard single-site systems operating within authority B's network have no basis for elevated alerting. This is precisely the fourth failure mode identified in Section 1: the administrative boundary between the two authorities prevents context from propagating through conventional means.

The federated architecture propagates the threat embedding of the identified individual across the administrative boundary via the central aggregator, without transmitting raw video between jurisdictions. When the VideoMAE v2 appearance embedding of a track in authority B's network exceeds the match threshold against the stored threat embedding, the prior local anomaly score from authority A's observation is incorporated into the ongoing trajectory score. The cross-jurisdiction handoff is seamless from the operator's perspective while remaining compliant with data-sharing restrictions between administrative domains.

6. Limitations and Open Questions

6.1. Conceptual Status of the Framework

As with the prior single-site work [15], this paper presents an architectural proposal without experimental validation. Hyperparameter choices — fusion window sizes, match probability thresholds, Anetwork baseline parameters, federated aggregation frequency — are unspecified and will require systematic empirical investigation.

6.2. Absence of City-Scale Multi-Modal Threat Trajectory Benchmarks

No public dataset provides annotated multi-camera threat trajectories at urban scale across heterogeneous sensor modalities. The construction of such a dataset — whether from synthetic city simulators, privacy-anonymised real data, or a combination — is a prerequisite for empirical evaluation and represents a significant community effort in its own right.

6.3. Scalability of the Dynamic Topology Graph

The proposed two-layer graph must update continuously as mobile nodes enter and leave the network. At N = 10,000 nodes — a plausible figure for a medium-sized city — the computational cost of graph neural network inference over the full topology requires careful engineering. Hierarchical graph partitioning, where city districts form super-nodes with internal topology abstracted, is one candidate solution; its impact on anomaly detection accuracy is unknown.

6.4. Re-Identification Across Extreme Appearance Change

The concern raised in prior work [15] — that clothing change defeats appearance-based Re-ID — is amplified at city scale, where trajectories span hours rather than minutes. Biomechanical embeddings based on skeletal pose estimation [13, 14] remain the most promising mitigation, but their effectiveness over multi-hour gaps with significant variation in walking surface, clothing weight, and physical exertion has not been demonstrated.

6.5. Cross-Modal Fusion Reliability

The temporal co-occurrence alignment proposed for heterogeneous sensor fusion is sensitive to clock drift between administrative domains. A GPS-anchored time synchronisation protocol is assumed but not specified. In its absence, a tolerance model that degrades match confidence gracefully with increasing temporal uncertainty would be required.

6.6. Ethical and Legal Dimensions at Government Scale

City-scale surveillance using AI trajectory aggregation raises concerns that exceed those of single-site deployment. Tracking individuals across an entire city over hours approaches the capability of mass surveillance, with well-documented potential for misuse [19]. Architectural privacy controls — on-device processing of raw video, transmission of embeddings rather than biometric data, mandatory retention limits on trajectory records — are not optional features but design requirements. The cross-jurisdiction propagation mechanism specifically requires the definition of bilateral data governance agreements specifying what constitutes permissible transmitted information, retention limits on threat embeddings, and oversight mechanisms for cross-domain matching. The framework as described requires the definition of explicit data governance policies at each level of the hierarchy before any real-world deployment could be considered responsible.

7. Conclusion

City-scale calibration-free threat trajectory aggregation is a problem of qualitatively greater difficulty than its single-site counterpart. The transition from a bounded camera network to a heterogeneous urban sensor ecosystem invalidates four core assumptions of single-site architectures: static topology, centralised processing, video as the sole modality, and membership within a single administrative domain. This paper has identified these failure modes, proposed a five-level federated framework to address them, and extended the three-component anomaly decomposition of prior work with a fourth network-level component for coordinated multi-actor threat detection.

The primary conceptual contributions are the dynamic topology graph, which replaces static camera adjacency maps with a live two-layer structure capable of incorporating mobile sensing units; the federated inference architecture, which enables city-scale deployment within realistic bandwidth and data-sovereignty constraints; the cross-modal fusion mechanism, which integrates video, acoustic, license plate, and access-control signals without requiring metric inter-modal calibration through a transformer-based architecture preferred over late fusion and strict attention bottlenecks for its robustness to unaligned modalities; the cross-jurisdiction propagation mechanism, which enables threat context to traverse administrative boundaries via embedding transmission rather than raw data sharing; and the strengthened formulation of Anetwork, which distinguishes coordinated multi-actor threats from coincidental convergence by jointly measuring spatial origin diversity and temporal synchronisation tightness.

Three urban threat scenarios illustrate that the framework would, conceptually, detect threats invisible to single-site analysis: multi-hour reconnaissance trajectories assembled from cross-jurisdictional fragments, coordinated infiltrations detectable only through network-level anomaly scoring, and cross-domain handoffs enabled by federated embedding propagation. Experimental validation of these claims, construction of a city-scale multi-modal threat trajectory benchmark, and the development of appropriate data governance frameworks are identified as the primary directions for future work.

References:

1. Feichtenhofer C., Fan H., Malik J., He K. SlowFast networks for video recognition // IEEE ICCV. — 2019. — P. 6202–6211.
2. Liu Z., Ning J., Cao Y. et al. Video Swin Transformer // CVPR. — 2022. — P. 3202–3211.
3. Wang L., Huang B., Zhao Z. et al. VideoMAE V2: Scaling video masked autoencoders with dual masking // CVPR. — 2023. — P. 14549–14560.
4. Wojke N., Bewley A., Paulus D. Simple online and realtime tracking with a deep association metric // ICIP. — 2017. — P. 3645–3649.
5. Ye M., Shen J., Lin G. et al. Deep learning for person re-identification: A survey and outlook // IEEE TPAMI. — 2022. — Vol. 44 (6). — P. 2872–2893.
6. He L., Wang Y., Liu W. et al. Foreground-aware Pyramid Reconstruction for alignment-free occluded person re-identification // ICCV. — 2019. — P. 8450–8459.
7. Ristani E., Solera F., Zou R. et al. Performance measures and a data set for multi-target, multi-camera tracking // ECCV. — 2016. — P. 17–35.
8. Sultani W., Chen C., Shah M. Real-world anomaly detection in surveillance videos // CVPR. — 2018. — P. 6479–6488.
9. Tian Y., Pang G., Chen Y. et al. Weakly-supervised video anomaly detection with robust temporal feature magnitude learning // ICCV. — 2021. — P. 4975–4984.
10. Jocher G. et al. Ultralytics YOLOv8. — 2023. — URL: https://github.com/ultralytics/ultralytics.
11. Zhang Y., Sun P., Jiang Y. et al. ByteTrack: Multi-object tracking by associating every detection box // ECCV. — 2022. — P. 1–21.
12. Beltagy I., Peters M. E., Cohan A. Longformer: The long-document transformer // arXiv:2004.05150. — 2020.
13. Xu Y., Zhang J., Zhang Q., Tao D. ViTPose: Simple vision transformer baselines for human pose estimation // NeurIPS. — 2022. — Vol. 35.
14. Starodubtsev I. S. Models, algorithms and software complex for building natural human-computer interaction based on gestures: PhD thesis. — 2024.
15. Адда-Аббу, А.-Р. Многокамерное слияние без калибровки для обнаружения угроз в системах видеонаблюдения: концептуальная архитектура

на основе глубокого обучения / А.-Р. Адда-Аббу // Молодой ученый. — 2026. — № 14 (617). — С. 3–8. — URL: https://moluch.ru/archive/617/134970.
16. McMahan B., Moore E., Ramage D. et al. Communication-efficient learning of deep networks from decentralized data // AISTATS. — 2017. — P. 1273–1282.
17. Kazemi S. M., Goel R., Jain K. et al. Representation learning for dynamic graphs: A survey // JMLR. — 2020. — Vol. 21 (70). — P. 1–73.
18. Nagrani A., Yang S., Arnab A. et al. Attention bottlenecks for multimodal fusion // NeurIPS. — 2021. — Vol. 34.
19. Zuboff S. The Age of Surveillance Capitalism. — New York: PublicAffairs, 2019.

Применение параметрических алгоритмов на BIM-платформах для повышения эффективности архитектурного проектирования

Васильева Анастасия Алексеевна, студент магистратуры
Чувашский государственный университет имени И.Н. Ульянова (г. Чебоксары)

В статье исследуются современные подходы к параметрическому моделированию в архитектурном проектировании с использованием технологий информационного моделирования зданий (BIM). Работа посвящена анализу инструментов и методов, позволяющих архитекторам создавать сложные динамические формы и оптимизировать проектные решения на всех этапах жизненного цикла объекта.

Ключевые слова: *параметрическое моделирование, BIM-технологии, архитектурное проектирование, параметрические семейства, автоматизация проектирования, информационное моделирование зданий.*

Современные архитектурно-строительные проекты требуют высокой точности, скорости разработки и экономической эффективности. Традиционные методы проектирования часто не позволяют оперативно анализировать множество вариантов и учитывать все взаимосвязи между элементами здания. В этих условиях параметрическое моделирование на базе BIM становится ключевым инструментом, позволяющим не только создавать сложные динамические формы, но и оптимизировать проектные решения на всех этапах жизненного цикла объекта. После перехода в проектирование в трехмерном пространстве, архитекторы всего мира стали искать новые возможности, которые позволили бы придать выразительности, плавности и порой воздушности объектам, чтобы создавать не только место для работы и отдыха, но и подчеркнуть уникальность каждого здания и сооружения.

Актуальность исследования обусловлена тем, что в современной архитектурной практике всё чаще реализуются объекты с нестандартной геометрией, что существенно ограничивает применимость традиционных методов проектирования. Одновременно повышается запрос со стороны заказчиков на гибкость и вариативность — требуется оперативно генерировать несколько вариантов проекта с детальным сопоставлением их технико-экономических показателей. Важным стимулом к внедрению новых подходов становится необходимость снижения количества ошибок: автоматизация расчётов и проверок в BIM-среде позволяет минимизировать влияние человеческого фактора и заметно сократить затраты на последующую доработку проектной документации. Кроме того, параметрическое моделирование выступает фундаментальной основой для интеграции в архитектурный процесс передовых технологий — таких как генеративный дизайн, искусственный интеллект и машинное обучение.

Цель работы заключается в комплексном исследовании методов и инструментов параметрического моделирования на базе BIM для архитектурного проектирования. Исследование направлено на анализ принципов интеграции параметрических методов в BIM среду, а также выявление преимуществ и ограничений использования параметрических моделей при проектировании сложных архитектурных объектов.

Параметрическое моделирование — метод проектирования, в основе которого лежит использование параметров элементов, являющихся составной частью общей модели, а также соотношения между этими параметрами, определяющие геометрическую форму модели. Изменения одного параметра автоматически приводят к корректировке всей модели.

Основные принципы параметрического моделирования:

— Объектно-ориентированность: каждый элемент модели — самостоятельный объект с набором свойств.
— Ассоциативность: связь между элементами модели, обеспечивающая автоматическое обновление при изменениях.
— Параметризация: задание зависимостей между параметрами через формулы и алгоритмы.
— Иерархия: структурирование модели по уровням сложности. Методы параметрического моделирования представляют собой различные под-

ходы к созданию цифровых моделей, в которых элементы связаны между собой определёнными зависимостями:

— Геометрическая — основан на задании геометрических зависимостей между элементами модели. В рамках этого подхода проектировщик определяет ключевые параметры: размеры, углы, расстояния и пропорции между объектами. При изменении любого из этих параметров система автоматически корректирует связанные с ним элементы. Такой метод особенно удобен на ранних стадиях проектирования, когда часто меняются базовые габариты и компоновка.
— Табличная — заключается в задании параметров через таблицы и базы данных. Вместо прямого редактирования геометрии пользователь работает с табличными формами, где перечислены характеристики элементов, их количество, материалы и прочие свойства. Этот подход удобен для управления спецификациями материалов, составления ведомостей объёмов работ и работы с каталогами типовых элементов.
— Физико-механическая — учитывает физические характеристики объектов. В рамках этого метода в модель закладываются параметры нагрузок, деформаций, теплотехнических и акустических свойств материалов. Это позволяет проводить инженерные расчёты прямо в среде проектирования: например, оценить, как изменение толщины стены повлияет на теплопотери здания, или как перераспределение нагрузок скажется на прочности конструкции.

Каждый из этих методов может применяться как самостоятельно, так и в комбинации друг с другом — в зависимости от задач проекта и стадии проектирования. Совместное использование разных подходов к параметризации повышает гибкость и точность моделирования, позволяя создавать сложные, адаптивные и оптимизированные архитектурные решения.

Преимущество BIM заключается в создании единой цифровой среды: все участники проекта — от архитектора до подрядчика — работают с общей виртуальной моделью объекта. Это устраняет фрагментацию данных: вместо разрозненных чертежей и сопроводительных документов формируется целостная информационная структура, доступная каждому участнику в режиме реального времени. Интеграция расчётов и смет в BIM-модель позволяет архитекторам принимать обоснованные проектные решения с учётом бюджетных ограничений и функциональных целей объекта. Например, анализ стоимости материалов в рамках модели помогает выбрать экономически эффективные решения, а возможность интеграции технологий.

Практическая реализация: оптимизация планировки здания архитектурного бюро

Задача: оптимизировать планировку здания по критериям:

— удобное расположение помещений на небольшой территории;

— соблюдение норм инсоляции;

— минимизация площади коридоров;

— обеспечение пожарной безопасности.

Перспективы развития:

— интеграция с инструментами генеративного дизайна;

— использование машинного обучения для прогнозирования оптимальных параметров;

— расширение критериев оптимизации (энергоэффективность, стоимость жизненного цикла).

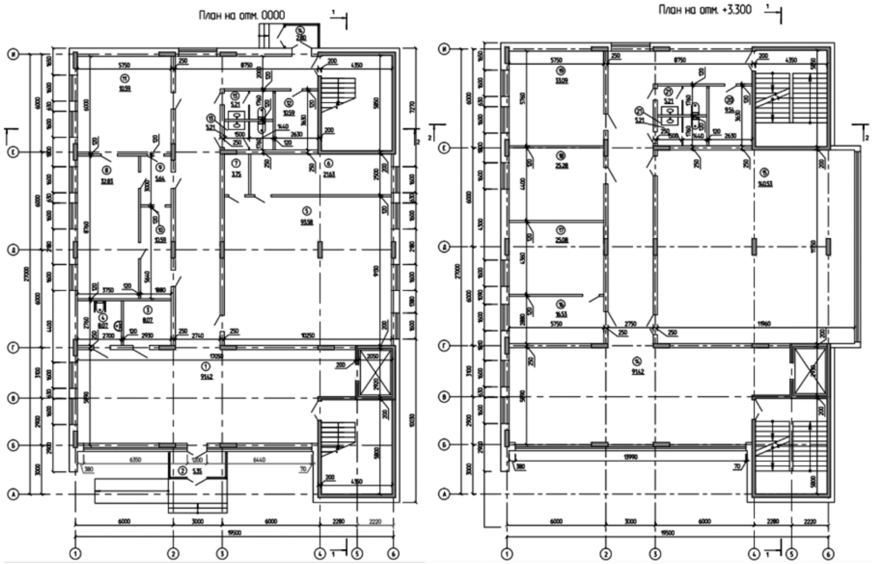

Рис. 1. **Настройка параметрической модели**

Рис. 2. **Конечный результат**

Исследование инструментов и методов параметрического моделирования на базе BIM отвечает актуальным потребностям архитектурной практики, способствует развитию цифровых компетенций отрасли и создаёт основу для внедрения передовых проектных решений. Его результаты будут полезны как для научных изысканий, так и для практического применения в проектных бюро, строительных компаниях и органах градостроительного регулирования. Внедрение параметрического моделирования в BIM-среде позволяет не только создавать сложные архитектурные формы, но и системно оптимизировать проект по множеству критериев. Это повышает конкурентоспособность проектных организаций, снижает риски и способствует реализации устойчивых, экономически эффективных решений.

В ходе исследования подтверждена высокая эффективность оптимизации проектных решений в архитектуре с использованием параметрических алгоритмов на базе BIM платформ.

Литература:

1. Шестопалов Е. В. и др. BIM технологии: учебное пособие. — Курск: ЮЗГУ, 2022;
2. Плешивцев А. А. Технология BIM-проектирования архитектурных объектов//Русайнс, 2023;

3. Алгоритмическое проектирование и визуальное программирование Георгиев Н. Г., Шумилов К. А., Семенов А. А. Визуальное программирование в задачах моделирования строительных конструкций // КиберЛенинка, 2021;
4. Семенов А. А. Автоматизированное моделирование оболочечных конструкций в Autodesk Revit с использованием Dynamo// Материалы конференций СПбГАСУ, 2022;
5. Клюев А. А. Исследование обработки данных в BIM-системах //УрФУ, 2025;
6. Савкин А. Н. Параметризация архитектурных решений в BIM-среде проектирования. // Экономика строительства и природопользования, 2023;
7. Кравченко Г. М., Подолько К. П., Литовченко Т. А. Дигитальная архитектура // Инженерный вестник Дона, 2017, № 4.
8. Т. А. Агасиев, Н. П. Гвоздев, А. П. Карпенко Новый подход к настройке Гауссовой суррогатной модели целевой функции в задаче параметрической оптимизации проектных решений //Вестник МГТУ им. Н. Э. Баумана. Сер. Приборостроение,2023, № 3 Маршак С. Я. Вот какой рассеянный. — М.: АСТ, 2016.
9. Чуковский К. От двух до пяти. — М.: Детская литература, 2017.

АРХИТЕКТУРА И СТРОИТЕЛЬСТВО

Переходные конструкции в высотном строительстве: принципы работы и обеспечение безопасности

Долгова Анастасия Дмитриевна, студент магистратуры
Чувашский государственный университет имени И. Н. Ульянова (г. Чебоксары)

В статье рассматриваются виды переходных конструкций, их роль в перераспределении нагрузок и обеспечении пространственной жесткости высотных зданий. Автор исследует влияние вертикальных и горизонтальных нагрузок на работу переходных ярусов.

Ключевые слова: *высотные здания, переходные конструкции, аутригерные системы, жесткость, безопасность.*

Современное высотное строительство характеризуется усложнением объемно-планировочных решений. Как подчеркивает В. Р. Мустакимов [17], организация переходных зон продиктована не только архитектурным обликом, но и функциональной неоднородностью здания на разных уровнях. Переходный этаж представляет собой зону концентрации несущих конструкций, обеспечивающую передачу усилий от элементов одной системы (например, часто расположенных пилонов жилой части) на элементы другой (редкие мощные колонны общественных пространств или стилобата).

Классификация и конструктивные особенности переходных систем

Выбор рациональной схемы является определяющим фактором для обеспечения устойчивости к эксплуатационным нагрузкам [10]. В практике проектирования выделяют четыре основных типа конструкций:

Переходные плиты. Массивное монолитное перекрытие увеличенной толщины. Монолитное исполнение является приоритетным, так как обеспечивает неразрезность системы и жесткое сопряжение с вертикальными элементами, минимизируя деформации в зонах продавливания [16].

Переходные балки и балки-стенки. Применяются для перекрытия значительных пролетов. Стальные балки эффективны при максимальных пролетах, а композитные (сталежелезобетонные) позволяют оптимизировать габариты за счет совместной работы стали на растяжение и бетона на сжатие.

Переходные стены. Работают как мощные связевые элементы и жесткие диафрагмы, что критически важно для зданий с консольными выносами [3].

Переходные раскосы. Использование раскосных систем позволяет оптимизировать распределение осевых усилий и снизить материалоемкость узла [12].

Таблица 1. **Сравнительный анализ технических характеристик переходных систем**

Тип конструкции	Преимущества	Основные ограничения	Область применения
Переходная плита	Высокая жесткость, простота планировки вышележащих этажей, эффективное распределение нагрузок [16].	Высокий собственный вес, большой расход бетона и арматуры, значительная экзотермия при бетонировании.	Здания со сложной сеткой колонн, жилые комплексы над торговыми центрами.
Переходные балки и балки-стенки	Меньший вес по сравнению с плитой, высокая изгибная жесткость при перекрытии больших пролетов.	Ограничение высоты помещений на техническом этаже, сложность армирования узлов сопряжения.	Переход от каркасной системы к разреженной сетке колонн (стилобаты, паркинги).
Переходные раскосы	Максимальная экономия материалов, высокая эффективность при работе на растяжение-сжатие [12].	Сложность узловых соединений, необходимость огнезащиты стальных элементов, высокая трудоемкость монтажа.	Сверхвысокие здания, аутригерные пояса, консольные выносы фасадов.
Переходные стены	Исключительная жесткость на всю высоту этажа, минимизация деформаций консолей [3].	Жесткая привязка к архитектуре (стена становится препятствием для свободной планировки).	Здания с выраженными консолями, переход от стеновой системы к каркасу.

Статическая работа и влияние вертикальных нагрузок

Процесс функционирования переходных конструкций включает восприятие концентрированных усилий, трансформацию напряженно-деформированного состояния (НДС) и передачу трансформированной нагрузки на основание.

Вертикальные нагрузки в высотных зданиях достигают колоссальных значений. На уровне переходного этажа эти усилия концентрируются в точках опирания вышележащих колонн. Для предотвращения хрупкого разрушения [продавливания] применяются принципы локального усиления: установка поперечной арматуры или жестких стальных вставок.

Взаимодействие с горизонтальными нагрузками и аутригерные системы

Роль переходных конструкций в восприятии ветровых и сейсмических нагрузок является критической. В рамках общей схемы они выполняют функции горизонтальных диафрагм жесткости.

Особое значение имеет внедрение аутригерных систем (высоких ферм или балок-стенок), которые жестко связывают центральное ядро с периметральными колоннами. Это создает значительное «плечо» внутренней пары сил, что:

— Кратно повышает изгибную жесткость каркаса.

— Снижает расчетный изгибающий момент в основании ядра на 25–40%.

— Ограничивает ускорение горизонтальных колебаний до нормативных 0,1 м/с^2, обеспечивая динамический комфорт [5, 15].

Конструктивная безопасность и защита от обрушения

Переходный этаж — это зона «скачка жесткости» [1]. При сейсмических воздействиях это создает риск формирования «мягкого этажа». Для нейтрализации рисков переходные плиты проектируются как абсолютно жесткие диски, выравнивающие инерционные силы [13].

В сценариях аварийных воздействий (взрыв, пожар) переходная конструкция должна обеспечивать живучесть системы. Если одна из опор нижнего яруса выходит из строя, плита начинает работать по принципу «мембраны» или мостового пролета, «подвешивая» нагрузку вышележащих этажей и предотвращая лавинообразное обрушение [16, 17].

Цифровая трансформация и методы расчета

Современное проектирование базируется на методе конечных элементов (МКЭ) в комплексах SCAD и LIRA-SAPR. Детальный анализ требует сгущения сетки в зонах опирания колонн и учета стадийности возведения, так как НДС плиты меняется по мере роста этажности. Интеграция BIM-технологий позволяет создавать цифровые двойники для непрерывного мониторинга состояния переходных зон на этапе эксплуатации [14].

Заключение

Переходные конструкции эволюционировали из вспомогательных элементов в многофункциональные интеллектуальные узлы. Применение высокопрочных бетонов (B40 и выше) и арматуры класса A500С в сочетании с аутригерными поясами позволяет возводить объекты любой сложности, гарантируя их долговечность и устойчивость к экстремальным воздействиям.

Литература:

1. Бекмаматова, Л. Н. Особенности оценки ветрового воздействия на высотные здания / Л. Н. Бекмаматова, В. Н. Алексеенко, О. Б. Жиленко // Молодежный научный форум: технические и математические науки. — 2016. — № 1 (30). — С. 4–12. — EDN VHEWRD. URL: https://www.elibrary.ru/item. asp?id=25279335
2. Скрипченкова, С. Ю. Воздействие ветровых нагрузок на высотные здания / С. Ю. Скрипченкова // Астраханский вестник экологического образования. — 2017. — № 2 (40). — С. 103–108. — EDN YSRJMT. — URL: https://www.elibrary.ru/item.asp?id=29368380
3. Павлушкин, М. Е. Разработка конструкции консольной части здания / М. Е. Павлушкин, С. С. Зимин // Неделя науки СПбПУ: материалы научной конференции с международным участием, Инженерно-строительный институт. В 3 ч., Санкт-Петербург, 18–23 ноября 2019 года / отв. ред. Н. Д. Беляев, В. В. Елистратов. Том Ч. 2.. — Санкт-Петербург: Федеральное государственное автономное образовательное учреждение высшего образования «Санкт-Петербургский политехнический университет Петра Великого», 2019. — С. 131–133. — EDN BNHEPI. — URL: https://www.elibrary.ru/item.asp?edn=bnhepi
4. Фотиева, В. А. Фундаменты высотных зданий / В. А. Фотиева, А. А. Столбикова, В. И. Пахолько // Наука. Техника. Технологии (политехнический вестник). — 2023. — № 2. — С. 88–90. — EDN ZYJRSV. https://elibrary.ru/item. asp?id=54805093
5. Сойту, Н. Ю. Влияние ветровых нагрузок на конструирование высотных зданий / Н. Ю. Сойту // Modern Science. — 2020. — № 2–1. — С. 393–396. — EDN RRPUXB. https://elibrary.ru/item. asp?id=42416116
6. Квадрициус, С. В. Основные проблемы, возникающие при строительстве высотных зданий в России / С. В. Квадрициус // Аллея науки. — 2023. — Т. 1, № 6 (81). — С. 251–254. — EDN RHCLKW. https://elibrary.ru/item.asp?id=54364338
7. Лавреев, А. Ю. Развитие мировой технологии возведения высотных зданий / А. Ю. Лавреев // Science Time. — 2016. — № 4 (28). — С. 462–466. — EDN VXDAJD. https://elibrary.ru/item.asp?id=26007231
8. Клименко, О. А. Сравнение свайных, плитных и комбинированных фундаментов для высотных зданий / О. А. Клименко // Инновационный потенциал развития общества: взгляд молодых ученых: сборник научных

статей 6-й Всероссийской научной конференции перспективных разработок, в 4-х томах, Курск, 01 декабря 2025 года. — Курск: Закрытое акционерное общество «Университетская книга», 2025. — С. 298–300. — EDN XXWQLD. https://www.elibrary.ru/item. asp?id=87345059

9. Сверчкова, Н. А. Влияние ветровой нагрузки на высотные здания / Н. А. Сверчкова, И. С. Казакова // Будущее науки-2017: Сборник научных статей 5-й Международной молодежной научной конференции: в 4-х томах, Курск, 26–27 апреля 2017 года / Ответственный редактор Горохов А. А.. Том 3. — Курск: Закрытое акционерное общество «Университетская книга», 2017. — С. 290–293. — EDN YQLGRF. https://elibrary.ru/item. asp?id=29266248
10. Сылка, Д. В. Особенности конструктивных схем каркасных высотных зданий / Д. В. Сылка, И. В. Ковалева, Д. Г. Злая // Наука. Техника. Технологии (политехнический вестник). — 2021. — № 4. — С. 188–194. — EDN YKLSKR. https://elibrary.ru/item. asp?id=47970615
11. Параметрическое моделирование сложной геометрии высотного здания: анализ влияния ветровой нагрузки и оптимизация / Е. Н. Облетов, Е. Д. Шаханов, М. А. Каргапольцева, С. С. Шилов // Приволжский научный журнал. — 2024. — № 1 (69). — С. 278–285. — EDN FLCLWZ. https://elibrary.ru/item. asp?id=65395554
12. Чернова, А. Н. Анализ использования переходных раскосов в высотном здании / А. Н. Чернова // Инновационные идеи молодых исследователей: Сборник научных статей по материалам XII Международной научно-практической конференции, Уфа, 13 июня 2023 года. — Уфа: Общество с ограниченной ответственностью «Научно-издательский центр «Вестник науки», 2023. — С. 309–314. — EDN IIHMGP. https://elibrary.ru/item. asp?id=54155328
13. Корабликова Юлия Константиновна, Грачев Григорий Денисович Анализ проблем и особенностей проектирования современных высотных зданий с учетом сейсмического воздействия // Вестник науки и образования. 2017. № 11 (35). URL: https://cyberleninka.ru/article/n/analiz-problem-i-osobennostey-proektirovaniya-sovremennyh-vysotnyh-zdaniy-s-uchetom-seysmicheskogo-vozdeystviya
14. Integrating BIM Technology in High-Rise Building Construction / ACE (Architecture and Civil Engineering) // Proceedings of the International Conference on Architecture and Civil Engineering. — 2025. — Vol. 15. — URL: https://www.ewadirect.com/proceedings/ace/article/view/25441

15. Abdelbasset, Y. M. High-Rise Buildings with Transfer Floors: Drift Calculations / Y. M. Abdelbasset, E. Y. Sayed-Ahmed, S. A. Mourad // IABSE Symposium Report. — 2014. — Vol. 102. — P. 637–644. — URL: https://www.academia.edu/48885134/High_Rise_Buildings_with_Transfer_Floors_Drift_Calculations
16. The Institution of Structural Engineers. Design of transfer slabs / The Institution of Structural Engineers. — London: IStructE, 2021. — URL: https://www.istructe.org/resources/guidance/design-of-transfer-slabs/
17. Мустакимов, В. Р. Проектирование зданий. Высотные здания: учебник для среднего профессионального образования / В. Р. Мустакимов. — 3-е изд. — Москва: Издательство Юрайт, 2026. — 291 с. — (Профессиональное образование). — ISBN 978–5–534–19663–4. — Текст: электронный // Образовательная платформа Юрайт [сайт]. — URL: https://urait.ru/bcode/590369

ТЕХНИЧЕСКИЕ НАУКИ

Gas Turbine Technology Trends and Thermo-Mechanical Durability Assessment of Hot-Section Components

Hadeel Raheem Jasim, PhD, Lecturer;
Hadeel Abdul Hassan Rahayf, PhD, Lecturer;
Mudher Naeem Yasir, PhD, Lecturer
University of Al-Qadisiyah (Diwaniya, Iraq)

The gas turbines are still significant to large-scale dispatchable power since they have high specific power, rapid start-up, and effective combined-cycle integration. At the same time, higher firing temperature, higher efficiency, flexible operation, and wider fuel adaptability increase the thermo-mechanical loading of hot-section components. This paper is a synthesis of a brief review of the development of gas-turbines with a focused analysis of hot-section durability assessment, particularly in turbine discs. A workflow of thermo-mechanical durability is outlined, and an enhanced deformation criterion is proposed. The method retains the structure of an adopted four-component cumulative damage model while improving sensitivity to cyclic and one-sided inelastic deterioration. Two validation cases show that the criterion preserves severity ranking and better distinguishes between one-sided creep-dominated and cyclic-creep-dominated regimes. In general, the findings suggest that the future development of gas-turbines will rely not only on the thermodynamic enhancement, but also on the more precise evaluation of the durability of hot-section elements.

Keywords: *gas turbine, hot-section durability, turbine disc, thermo-mechanical fatigue, creep-fatigue, cumulative damage, finite-element analysis*

1. Introduction

Gas turbines still take the center stage in the contemporary power systems due to their ability to produce high specific power, quick start-up, and seamless integration with combined cycle generation. These characteristics are important in systems where the proportion of variable renewable energy is increasing since there are still flexible thermal plants to maintain grid stability and dispatchable generation. Meanwhile, the more efficient heavy-duty gas turbines now are running at combined-cycle efficiencies well over 64 percent, which demonstrates that it is not yet a mature technology but one that is in continuous improvement [1, 2].

This progress, however, increases the demands on the hot section. Increased firing temperatures, enhanced thermal gradients, increased frequency of start-stop and load-following duty and increased range of fuel-flexibility targets increase the thermo-mechanical loading of blades, vanes, and discs. This has led to durability being a key design and life-management issue instead of a secondary verification process [3–7].

The present paper addresses this issue from two connected sides. First, it outlines the key development trends in gas turbines and their implications to the reliability of the hot-section. Second, it suggests a compact enhanced deformation-based criterion to assess turbine-disc durability and also studies its behavior using two validation cases [6, 8, 15].

2. Gas Turbine Development Trends, Durability Challenge, and Study Objective

Development of gas-turbines is now being guided by increased combined-cycle efficiency, high turbine inlet temperature, increased operational flexibility, broader fuel adaptability, and more data-based lifecycle management. In that respect, the modern heavy-duty gas turbine is more than a thermodynamic machine, it is a thermal, material and durability system. The evolution is as shown in Figure 1, and Table 1 connects the key development phases to their enabling technology and implication of durability.

The advancements have been based on the enhancement of aerodynamics, pressure ratio, combustion design, sealing, and integration of combined cycles. Meanwhile, the trend towards H-, J-, and HL-class machineries has created advanced cooling, single-crystal superalloys, and thermal barrier coatings as mandatory features rather than secondary improvements [2–4, 7]. Cooling remains a key limit since the gas temperatures are above the permissible temperatures of metal of many hot-section components [3]. Thermal barrier coating increases the usable thermal window but their decay is a significant issue [4,10]. The machines that run at higher temperatures also needs better oxidation resistance, creep strength, and microstructural stability [7].

Table 1. **Main stages and drivers of gas turbine technology development**

Stage / focus	Main technical objective	Key enabling technologies	Main durability implication
Classical industrial GT development	Higher simple-cycle power and reliability	Aerodynamic refinement, improved compressor/ turbine design	Moderate thermal loading, mainly stress-based design

Stage / focus	Main technical objective	Key enabling technologies	Main durability implication
Advanced combined-cycle era	Higher plant efficiency	Better exhaust heat recovery, higher pressure ratio, better combustion	Higher steady thermal stress in hot-section parts
High-temperature H/J/HL-class era	Efficiency beyond 60% CCGT and then above 64%	Advanced cooling, single-crystal alloys, TBCs, improved sealing	Stronger creep-fatigue interaction and coating life issues
Fuel-flexible / hydrogen-ready era	Lower carbon intensity with dispatchable generation	Low-NOx hydrogen-capable combustors, upgraded thermal management	Changed combustion temperature field and transient thermal risk
Digital lifecycle era	Reliability under flexible operation	Digital twins, diagnostics, prognostics, inspection-informed models	Life prediction becomes continuously updated rather than static

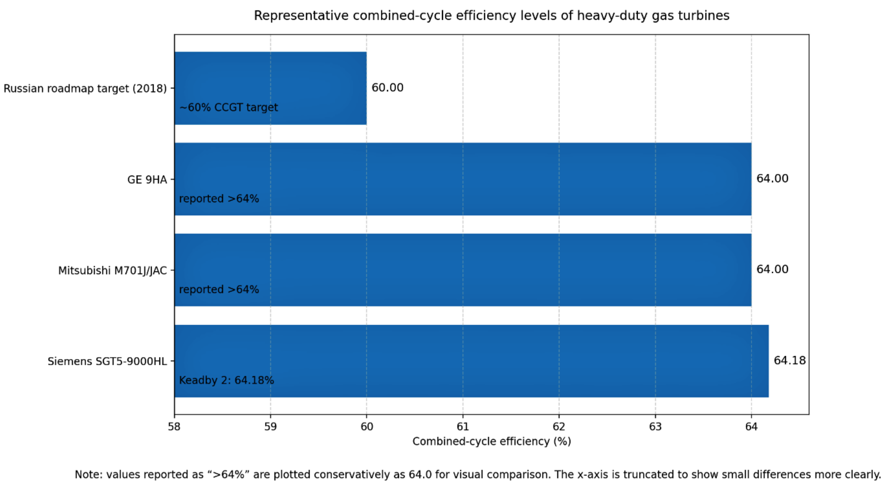

Fig. 1. **Representative heavy-duty gas turbine efficiency levels**

Fuel flexibility and lifecycle-oriented operation add further complexity. Gas turbines that can use hydrogen and the associated combustion systems are receiving growing interest since they can facilitate decarbonization while preserving dispatchability [5]. Simultaneously, gas turbines are being operated in more start-stop cycles, load following, and variable thermal histories, so the rotor life extension, assessing it with information in inspections, and digital twins to manage performance and health is of increasing interest [8,9].

In this wider evolution, one of the central technological bottlenecks is still the hot-section durability. Higher performance intensifies thermal gradients, inelastic strain, creep exposure, oxidation, and cyclic damage in the hottest and most highly loaded components. In the case of blades and vanes, the primary issues are heat loading, cooling performance, coating loss, thermo-mechanical fatigue, and, in certain instances, repair problems [10,11]. In discs and rotors, centrifugal stress, radial temperature gradients, start up/shut down transients, creep-fatigue interaction, and unidirectional inelastic accumulation are the leading problems. Thermal-gradient fatigue experiments also demonstrate that realistic high-temperature testing requires not only constitutive behavior, but imposition and measurement of temperature gradients in testing [12–14].

Two key gaps arise as a result of this background. First, most of the review papers explain the trends in technology neatly yet the linkage between development of gas turbines and lifing of components is implicit. Second, most of the detailed durability studies are done on material behavior, finite-element analysis, thermal-gradient tests, or crack-growth prediction, but there is no general linkage of these techniques to the broader evolution of modern gas turbines [6,8,12–14]. The use of deformation methods is meritorious since they differentiate between cyclic plasticity, cyclic creep, one-sided plastic accumulation, and one-sided creep accumulation [15]. Nevertheless, in cases where these mechanisms are only addited together via a linear sum, the model can be not sensitive enough to the actual thermo-mechanical regime.

This paper aims thus to relate the trends in gas-turbine technology to the assessment of durability of the hot-section and to suggest a compact enhanced deformation-based criterion that improves sensitivity to creep participation and one-sided inelastic accumulation.

3. Methodology

3.1. Thermo-mechanical durability workflow

Figure 2 summarizes the analytical procedure followed in this work. The workflow begins with the operating scenario which includes the start-up, load-following, steady high-temperature dwell, and shutdown. This cycle defines the thermal boundary conditions acting on the component. Finite element thermal and stress-strain analysis is then used to obtain the local temperature field, stress concentrations, and inelastic strain histories in the critical regions. Simultaneously, a constitutive material model, generally of elastic-plastic-creep or viscoplastic type, is employed to model the inelastic response of the material at temperature. The resultant measures of deformation are inputted into the damage criterion that yields a scalar index of severity for the considered loading regime. When necessary, the evaluation may be furthered to crack-growth or residual-life analysis. Validation is conducted using comparison with specimen tests, rig data, inspection or service observations, and digital updating can be a supplemental feedback phase.

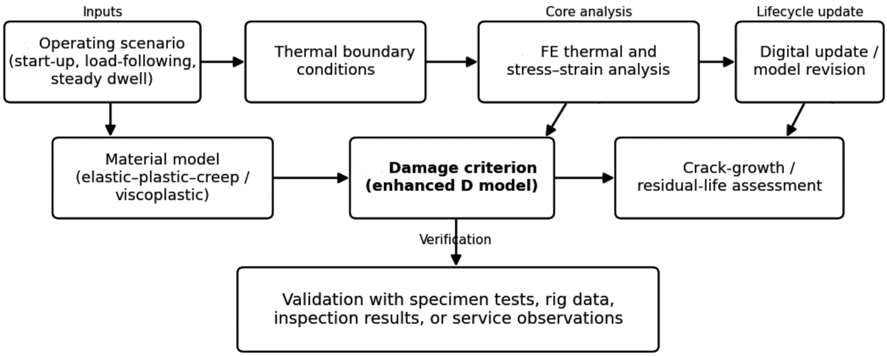

Fig. 2. **Compact workflow for thermo-mechanical durability assessment**

3.2. Classical and proposed enhanced criterion

In the case of hot-section components operating under non-isothermal cyclic loading, deformation-based descriptions are convenient since they conserve the separation of the primary damage channels. In the current study, the classical foundation will be assumed to be a four-component deformation based cumulative damage model of turbine discs as introduced in [15], wherein the cumulative damage is expressed as.

$$D = D_1 + D_2 + D_3 + D_4, \quad (1)$$

where D_1 represents cyclic plastic straining, D_2 — cyclic creep straining, D_3 — one-sided plastic accumulation, and D_4 — one-sided creep accumulation.

The appeal of this structure is that it isolates reversible cyclic inelasticity and progressive monotonic accumulation. Nevertheless, a pure linear combination is not always sensitive enough to the real loading regime, particularly when creep dominance or when one-sided accumulation becomes significant relative to the cyclic strain range. Because of this reason, the four-component model adopted is used here as the starting point for a compact enhanced criterion.

To maintain the clarity of the classical model and increase sensitivity of the mechanism, enhanced reduced terms are introduced. Let Δs_p and Δs_c refer to the equivalent cyclic plastic and cyclic creep strain ranges, and s^+_p and s^+_c refer to the one-sided accumulated strains. The modified partial contributions are given as

$$\tilde{D}_1 = D_1(1|a\frac{\Delta s_c}{\Delta s_p + \Delta s_c}), \quad (2)$$

$$\tilde{D}_2 = D_2(1|b\frac{s_c^+}{s_p^+ + s_c^+}), \quad (3)$$

$$\tilde{D}_3 = D_3(1|g\frac{s_p^+}{\Delta s_p + s_0}), \quad (4)$$

$$\tilde{D}_4 = D_4(1|d\frac{s_c^+}{\Delta s_c + s_0}), \quad (5)$$

where *a, b, g* and *d* are correction coefficients, s_0 — is a small regularization constant. These terms maintain the physical meaning of the original four components of damage but makes them more sensitive to mechanism interaction.

The total damage index is then defined as

$$D^* = q_1\tilde{D}_1 + q_2\tilde{D}_2 + q_3\tilde{D}_3 + q_4\tilde{D}_4 + \mu_{12}\sqrt{\tilde{D}_1\tilde{D}_2} + \mu_{34}\sqrt{\tilde{D}_3\tilde{D}_4}, \quad (6)$$

where q_1-q_4 are weighting factors and μ_{12}, μ_{34} characterize the interaction between the cyclic and monotonic damage channels.

3.3. Validation cases and coefficients

To conduct proof-of-concept assessment two representative cases were picked out of the rotating-disc dataset in [15] and referred to here as Case 1 and Case 2. These cases were selected since they are related to two distinctly different patterns of deterioration. Case 1 is dominated by one-sided creep accumulation and Case 2 is ruled mainly by cyclic-creep response.

For the validation calculations, the strain measures defined in Section 3.2. were used to evaluate the enhanced criterion.

For **Case 1**, the input values were

$$\Delta s_p = 0.06, \Delta s_c = 0.028, s_p^+ = 0.12, s_c^+ = 0.16.$$

For **Case 2**, the corresponding values were

$$\Delta s_p = 0.64, \Delta s_c = 0.350, s_p^+ = 0.89, s_c^+ = 0.79.$$

The adopted model coefficients were

$$a = 0.25,\ b = 0.30,\ g = 0.10,\ d = 0.10,$$

$$q_1 = 1.00,\ q_2 = 1.15,\ q_3 = 1.00,\ q_4 = 1.20,$$

$$\mu_{12} = 0.10,\ \mu_{34} = 0.15.$$

These values keep the enhanced model close to the classical structure but with a greater importance to creep-related deterioration.

4. Results and Discussion

The classical damage components (D_1–D_4) were selected from the rotating-disc results as the baseline in the selected validation cases. The enhanced quantities $\tilde{D}_1$–$\tilde{D}_4$ and the total enhanced damage D^* were then calculated in the present study using Eqs. (2) — (6). The overall outcomes are listed in Table 3.

Table 3. **Classical and enhanced damage indices for the selected validation cases**

Case	Level	D_1 / $\tilde{D}_1$	D_2 / $\tilde{D}_2$	D_3 / $\tilde{D}_3$	D_4 / $\tilde{D}_4$	Total damage	Governing mode
Case 1	Classical	0.0073	0.1010	0.0320	1.5700	D = 1.7100	—
Case 1	Enhanced	0.0079	0.1183	0.0384	2.4650	D^* = 3.1900	One-sided creep accumulation
Case 2	Classical	0.0530	0.6200	0.0700	0.2500	D = 1.0100	—
Case 2	Enhanced	0.0577	0.7074	0.0797	0.3064	D^* = 1.3600	Cyclic-creep response

Table 2 reveals that the two cases are not only different in the aggregate severity, but also in the internal structure of damage. In Case 1, the predominant contribution is $\tilde{D}_4$, which suggests that the regime is dominated by one-sided creep accumulation. Case 2, in its turn, is dictated mostly by $\tilde{D}_2$, which is an indication of a deterioration process that is controlled by cyclic and creep processes.

The overall effect of the enhanced formulation can be analyzed by drawing a comparison between the classical cumulative damage D and the enhanced total damage D^*. In the chosen cases, classical values are.

$$D_{\text{Case-1}} = 1.71,\ D_{\text{Case-2}} = 1.01,$$

while the corresponding enhanced values are

$$D^*_{\text{Case-1}} = 3.19,\ D^*_{\text{Case-2}} = 1.36,$$

Figure 3 presents these results as the comparative level of damages (classical and enhanced) in both cases.

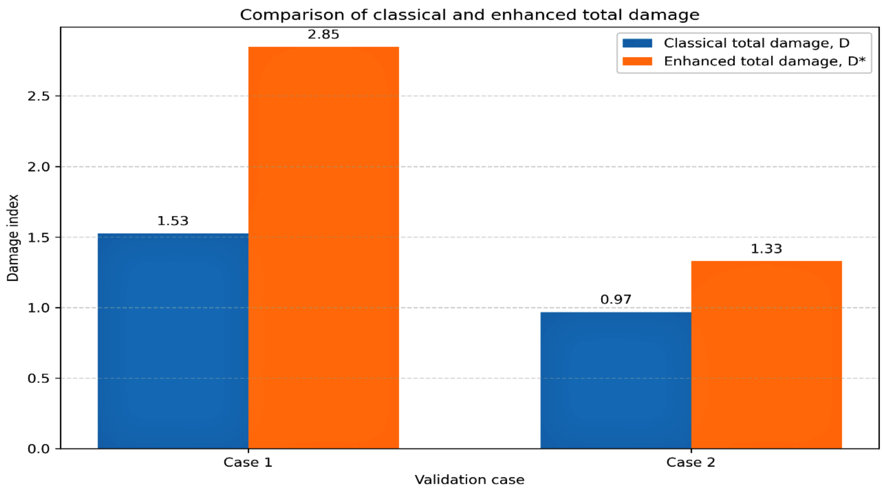

Fig. 3. **Comparison of classical and enhanced total damage for the selected validation cases**

There are two key effects as shown in Figure 3. First, the enhanced criterion keeps the severity ranking of the cases: Case 1 remains more critical than Case 2. This is necessary, as the physical order of deterioration states should not be distorted by an enhanced model. Second, the enhanced criterion increases the predicted severity in both cases, although not equally. This implies that the suggested formulation does not use a uniform correction. Rather, it reacts to the internal damage structure of every case in a different manner.

To bring this out better a factor of amplification can be given as

$$K_A = \frac{D^*}{D}.$$

For Case-1,

$$K_{A,\text{Case-1}} = \frac{3.19}{1.71} \approx 1.87,$$

while for cas-2,

$$K_{A,Case-2} = \frac{1.36}{1.01} \approx 1.35.$$

In this way, the enhanced model raises the severity estimate of Case 1 compared to Case 2, which is in line with the higher contribution of one-sided creep accumulation in Case 1. Generally, the proposed formulation maintains severity ranking, better mechanism discrimination, and is a conservative without physical interpretability loss. In particular, Case 1 is dominated by $\tilde{D}_4$, whereas Case 2 is dominated by $\tilde{D}_2$.

These results must be considered within the wider perspective of gas-turbine development. Higher firing temperature, operation flexibility, and increased fuel adaptability are all factors that increase thermo-mechanical stress on the components of the hot section. This is the reason why the trends in technology, discussed above, contribute to the necessity of more mechanism-sensitive models of durability. The overall finding is thus integrative: the development trends of gas turbines and durability modelling are not distinct issues, but two aspects of the same engineering challenge.

6. Conclusion

The paper has connected the development trends of gas-turbines with the hot-section durability assessment. The suggested reduced enhanced criterion maintained the severity ranking of the two validation cases and enhanced mechanism discrimination. Case 1 was dominated by $\tilde{D}_4$, which indicate one-sided creep accumulation, whereas Case 2 was dominated by $\tilde{D}_2$, which indicate a cyclic-creep-controlled regime. The total damage was also increased more by the enhanced model on Case 1 than on Case 2, which is also in line with the increased contribution of the one-sided creep accumulation.

In general, the findings indicate that the suggested formulation offers a more informative description of thermo-mechanical deterioration than a simple linear cumulative rule, while remaining compact enough for engineering use. Future work should be focus on broader calibration, fieldwise FE implementation, extension to other hot-section components and more integration with the crack-growth and lifecycle assessment.

References:

1. International Energy Agency (IEA). Electricity 2025. Paris, 2025. Available at: https://www.iea.org/reports/electricity-2025
2. Guinness World Records. Most Efficient Combined Cycle Power Plant. Verified for Keadby 2 at 64.18%, 2024. Available at: https://www.guinnessworldrecords.com

3. Zhu S., Li Y., Yan J., Zhang C. Recent advances in cooling technology for the leading edge of gas turbine blades. Energies, 2025, vol. 18, no. 3, art. 540.
4. Bogdan M., Peter I. A comprehensive understanding of thermal barrier coatings (TBCs): applications, materials, coating design and failure mechanisms. Metals, 2024, vol. 14, no. 5, art. 575.
5. ETN Global. Hydrogen Gas Turbines Report 2024. Brussels, 2024. https://etn. global/wp-content/uploads/2024/11/ETN-Global-Hydrogen-Gas-Turbines-Report-10–2024.
6. Moverare J., Lancaster R. J., Jones J. et al. A review of recent advances in the understanding of thermomechanical fatigue durability and failure mechanisms in nickel-based superalloys. Metallurgical and Materials Transactions A, 2025, vol. 56, pp. 1115–1134.
7. Gudivada G., Pandey A. K. Recent developments in nickel-based superalloys for gas turbine applications: review. Journal of Alloys and Compounds, 2023, vol. 963, art. 171128.
8. ETN Global. Rotor Lifetime Assessments: A Reference Report. Brussels, 2024. etn. global/wp-content/uploads/2024/05/ETN-Rotor-Lifetime-Assessments-A-Reference-Report-March-2024.
9. Farhat H., Altarawneh A. Physics-informed machine learning for intelligent gas turbine digital twins: a review. Energies, 2025, vol. 18, no. 20, art. 5523.
10. Vagge S. T., Ghogare S. Thermal barrier coatings: review. Materials Today: Proceedings, 2022, vol. 56, part 3, pp. 1201–1216.
11. Tan Q., Liu K., Li J., Geng S., Sun L., Skuratov V. A review on cracking mechanism and suppression strategy of nickel-based superalloys during laser cladding. Journal of Alloys and Compounds, 2024, vol. 1001, art. 175164.
12. Sun J., Yuan H., Vormwald M. Thermal gradient mechanical fatigue assessment of a nickel-based superalloy. International Journal of Fatigue, 2020, vol. 135, art. 105486.
13. Sun J., Yuan H. Investigation of thermal gradient mechanical fatigue test methods for nickel-based superalloys. Experimental Mechanics, 2021, vol. 61, no. 3, pp. 565–580.
14. Aublet A., Rambaudon M., N'guyen F., Ryckelynck D., Remacha C., Cariou R., Proudhon H. Mechanical fatigue testing under thermal gradient and manufacturing variabilities in nickel-based superalloy parts with air-cooling holes. Experimental Mechanics, 2022, vol. 62, no. 7, pp. 1079–1091.
15. Гецов Л. Б., Семенов А. С., Грищенко А. И., Игнатович И. А. Современные методики расчетного определения термоусталостной прочности лопаток

и дисков газовых турбин // LXV научно-техническая сессия по проблемам газовых турбин и парогазовых установок «Фундаментальные проблемы исследований, разработки и реализации научных достижений в области газовых турбин в российской экономике»: сборник докладов. Санкт-Петербург, 2018. С. 136–138.

Effect of silicon oxide addition on the corrosion resistance and contact angle of Ti15Mo alloy for biomedical applications

Saleh Jawad Hamza, PhD, lecturer;
Ahmed Mousa Marheb, PhD, lecturer
University of Al-Qadisiyah (Diwaniya, Iraq)

Study investigated the effect of sio_2 addition on the corrosion resistance and surface wettability of Ti-15Mo alloy for biomedical applications. The alloy was prepared by powder metallurgy using Ti and Mo powders, with sio_2 added in the range of 0.5–3 wt%. The powder mixture was blended for 5 h, compacted into disk-shaped samples under 800 mpa, and sintered at 950 °C at a heating rate of 10 °C/min during a period of 7 h. The influence of sio_2 was examined by X-ray analysis, corrosion testing, and contact angle measurement. The results showed that sio_2 addition had a great effect in enhancing the corrosion resistance of the Ti-15Mo alloy. The highest performance was achieved at 3 wt% sio_2, where the corrosion resistance was improved by 98.8% and the corrosion rate decreased to 2.31E-10 mpy when increasing the porosity up to 18.7%. The contact angle also decreased from 45.786° to 35.473°, indicating improved surface wettability. These results imply that Ti-15Mo alloy with the reinforcement of sio2 can be highly utilized as a biomaterial, particularly in orthopedic implant applications.

Keywords: *biomaterials, corrosion resistance, contact angle, orthopedics.*

1. Introduction

Since the 1980s, titanium and its alloys have found many applications in dentistry and orthopedic medicine due to their combination of several characteristics that are very desirable in biomedical applications, including strong corrosion resistance, excellent biocompatibility, low density, and suitable mechanical performance [1, 7, 8, 10, 15, 16]. Due to this combination, titanium-based materials have become particularly suitable to load-bearing applications, including dental prostheses and implants, joint replacements, and other orthopedic applications [7, 8, 11, 15].

Titanium has been of particular interest among the metallic biomaterials due to the generally more favorable biological response of titanium compared to several cobalt- and iron-based alloys. In such materials, elements like Co, Ni and Cr can be emitted in the forms of the ions within the body and will result in untoward biological effects [7, 8, 10, 15, 16]. Commercially pure titanium (CP-Ti) and most titanium alloys on the other hand have demonstrated good biocompatibility both in experimental and clinical practice [5, 7, 8, 10]. This tendency can be explained by the stable passive oxide coating which develops naturally on the surface of titanium and covers the material in physiological conditions [5].

Corrosion resistance is of particular importance to implant materials since the human body is a chemically aggressive environment. In body fluids, chloride ions, organic compounds and the other dissolved species are found and they may speed up the rate of electrochemical degradation [1, 14, 15, 19]. In the case of corrosion, the metal ions and the degradation products can be released into the surrounding tissue, thereby affecting the performance of the implants and increasing the disadvantage of the long-term biological response. For this reason, improving the corrosion resistance of titanium-based alloys remains one of the main goals of biomaterials research [7, 8, 10, 15, 16].

Simultaneously, the corrosion resistance of the implant does not determine its performance alone, but the properties of the surface also play a role. The contact between the implant surface and surrounding hard or soft tissue is the key factor in the process of osseointegration, soft-tissue attachment, and long-term stability [5, 6]. Over the past few years, surface and compositional modifications able to enhance wettability, better tissue response and lessen the risk of bacterial adhesion and peri-implant complications have received a growing interest [5, 6, 9].

Titanium is commercially available in the α-phase form, and it has been utilized successfully in several biomedical applications because of its excellent corrosion resistance and non-toxicity in the human body [1, 7, 10, 15]. Nevertheless, its mechanical characteristics do not always have the required strength and wear resistance as needed by applications [7, 10, 11]. Titanium alloys were developed as a result of this limitation. An example of one of the first and most commonly used is Ti-6Al-4V, providing better strength. Nevertheless, its elastic modulus remains significantly better than the natural bone [10, 11, 15, 16]. Such a discrepancy can lead to stress shielding that can lead to bone resorption and, ultimately, to loosening of the implants.

To address these shortcomings, recent research has been directed at finding new titanium-based biomaterials that have a lower elastic modulus, better corrosion resistance, and non-toxic alloying elements [10, 12, 15, 16, 17]. In this regard, molybdenum is considered an attractive β-stabilizing element to titanium alloys.

Ti-Mo systems have been of interest since they could offer a desirable trade-off between mechanical performance and biocompatibility relative to the traditional titanium alloys [10, 13, 16, 19]. However, the behavior of Ti — Mo alloys is strongly influenced by both their composition and the processing conditions. Previous studies have shown that Mo addition can enhance the development of phases like martensitic orthorhombic α″ and ω phases, which can raise the strength but at the same time raise the elastic modulus and and increase brittleness [16].

This is the reason that Ti-Mo alloys still require further modification to enhance their biomedical use. One possible route is the incorporation of ceramic oxides like SiO_2 which could improve the level of corrosion resistance and alter the behavior of surfaces. From this perspective, the current research is an exploration of Ti-15Mo alloy with SiO_2 and its possible usage in biomedical applications especially where better corrosion behavior and good surface characteristics are needed [13, 19].

2. Experimental Work

Ti-15Mo — $xSiO_2$ specimens were fabricated by powder metallurgy. The average particle size and purity of the starting powders are listed in Table 1. The weighted powders were meticulously mixed in a rotating automatic ball mill using steel balls of different diameters with ethanol serving as the wet medium of mixing. The mixing was conducted during 5 h to obtain a homogenous powder blend. After mixing, 3.5 g of the mixture was then pressed into disk-shaped specimens, 12 mm in diameter and 6 mm in thickness, using an electric hydraulic press. The compaction pressure was 800 Mpa, and the specimens were maintained at the pressure of 800 Mpa in 4 min. The green compacts were then sintered in an electric furnace under an argon atmosphere. The temperature was raised to 950 °C at a heating rate of 10 °C/min and the samples maintained at this temperature for a duration of 7 hours. The specimens were then allowed to cool in the furnace to allow them to attain room temperature after sintering.

Table 1. **Characteristics of the powders used in this study**

Powder	Average particle size (μm)	Purity (%)
Ti	26.43	99.85
Mo	29.89	99.90
SiO_2	53.433	99.95

2.1 Microstructures Characterization

X-Ray Diffraction. After sintering, The specimens of Ti-based alloys were analyzed via X-ray diffraction (XRD) and the data compared with the reference data. The measurements were conducted by using the Cu ka radiation having a wavelength of 1.54060 Å. The scan range was set at 20° — 80° with the step size of 0.02° and the scan speed was 6°/min. The instrument was working at 40 kV and 30 mA.

Microstructure Observation. After sintering, all the specimens were microstructurally examined through sequential grinding followed by 180, 400, 600, 800, 1000, 1200, 1500, and 2000-grit silicon carbide paper. The samples were then polished with diamond paste to obtain a smooth mirror like surface. Etching was performed at room temperature using the solution listed in Table 2. Following etching, they were rinsed in water and dried, and optical microscopy was performed at 400x magnification and scanning electron microscopy (SEM). Phase identification, grain morphology, grain size and grain-boundary features were studied using the microstructural analysis.

Table 2. **Composition of the etching solution**

Constituent	Amount (mL)
HF	10
HNO_3	5
H_2O	85

2.2 Corrosion Test

Polarization testing was used to determine the behavior of corrosion by a standard three electrode electrochemical cell in Ringer solution according to the ASTM standards [18]. The cell included the specimen as the working electrode, platinum as the working electrode, platinum was used as the auxiliary electrode, and a saturated calomel electrode acted as the reference electrode. Winking M Labf200 potentiostat was used to conduct the tests. Potentiometric polarization was performed after stabilization at the open-circuit potential 250 mV below the open-circuit potential to 800 mV above it. The potential was swept in the anodic direction and the resulting current response was recorded. Based on the polarization curves, corrosion potential (E_{corr}) and corrosion current density (I_{corr}) were calculated and the corrosion rate was calculated with the help of Equation (1) [18].

$$Corrosion\,Rate\ (mpy) = \frac{0.13\, I_{corr}\left(E.W.\right)}{\rho} \quad (1)$$

where $E.W.$ is the equivalent weight (g/equiv.), p is the density (g/cm^3), and I_{corr} is the corrosion current density (μA/cm^2).

2.3 Contact Angle Test

Contact angle inspection device measure the angle of contact between the liquid (Distilled water) and solid (Ti15Mo-X Sio2) alloys substrate to know the wettability of the electrolyte to the surface of the base sample.

3. Result And Discussion

3.1 Microstructure Characterization

The XRD of the green compact alloys reflect only the starting constituent phases i. e. titanium (Ti), molybdenum (Mo) and silicon oxide (SiO_2), as no phase change is experienced during compaction. These transformations are diffusion-controlled reactions and thus need high temperatures to occur. Figure 1 shows the XRD pattern of (Ti-15Mo) alloy with 3% SiO_2, which had been sintered at 950 °C during 7 h in an atmosphere of argon. The findings show that following sintering, the initial elemental (Ti) constituents were transformed to two titanium based solid-solution phases, α-Ti and β-Ti. The observed behavior proves that the chosen temperature of sintering and the holding time were adequate to facilitate interdiffusion among the alloying elements and to finalize the phase transformation process.

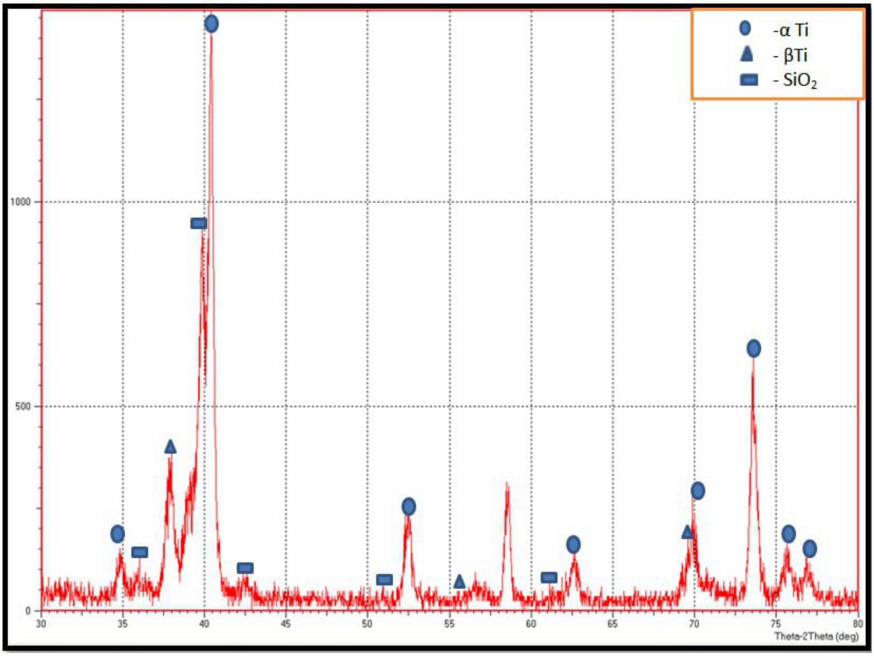

Fig. 1. **XRD pattern of Ti-15Mo-3SiO$_2$ alloy after the sintering process**

3.2. Microstructure Representation

The microstructure of the prepared specimens was observed under light optical microscopy (LO). Figure 2 presents optical micrograph of the base Ti-15Mo sintered alloy, as seen under 400x magnification. Within the etched surface, the grain boundaries and the phase contrast in the alloy are easily identified. The microstructure has a duplex morphology made by two different regions as in Figure 2. Brighter areas are the α -Ti phase and the darker areas are the β -Ti phase. This means that the sintered base alloy developed a typical α + β titanium microstructure. The distribution of phases observed also indicates that the powder metallurgy route offered a relatively uniform microstructure across the matrix. This type of microstructural uniformity is significant in that it may lead to predictable material behavior and preferential mechanical performance. Generally, the optical micrograph shows that the two-phase structure as desired in the Ti-15Mo base alloy was achieved successfully after the sintering.

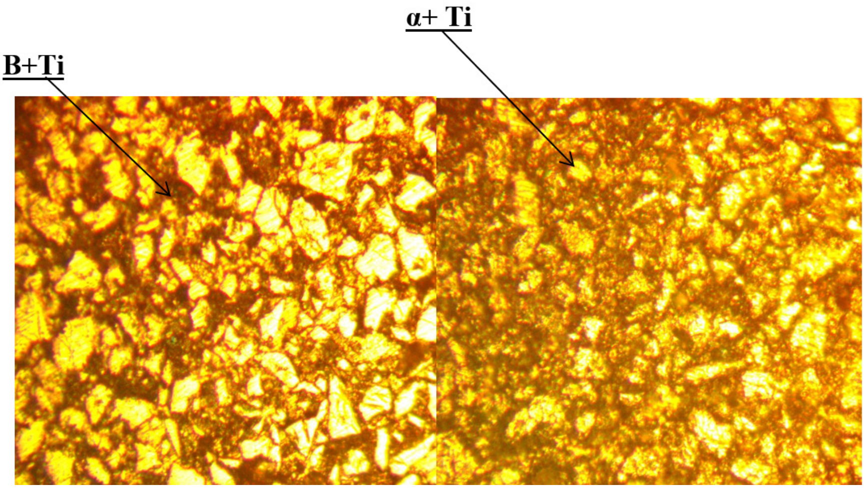

Fig. 2. **Optical micrograph of the base Ti-15Mo alloy at 400× magnification**

3.3. Contact Angle Test

When the percentage of silicon oxide increases, the contact angle decreases, and this means that the wettability increases, which leads to an increase in the bonding between body tissues and the implanted alloy and reduction of time required for healling. From Table 3 which is shown the variation of contact angles improvement with silicon oxide contents, we notic that there where an increament in improvement percentagre with increasing silicon oxide content, because of silicon oxide addition led to increase surface tension of surface alloy according to the following equation.

Table 3. **Contact angle values and percentage reduction for Ti-15Mo — xSiO_2 alloys**

Sample	Contact angle (°)	Reduction (%)
Base	45.794	—
0.5 wt% SiO_2	45.657	0.30
1.0 wt% SiO_2	42.239	7.76
1.5 wt% SiO_2	41.624	9.11
2.0 wt% SiO_2	39.528	13.68
2.5 wt% SiO_2	38.701	15.49
3.0 wt% SiO_2	35.168	23.20

3.4 Corrosion Test

The electrochemical testing of thecorrosion behavior of Ti-15Mo and Ti-15Mo — xSiO_2 alloys was done in the Hank solution at 37±1 °C. The related current-potential relationships, presented as polarization curves in Figure 3 and Figure 4 indicate both the anodic and cathodic responses of the studied alloys. The current dropped with the change in the potential to a minimum value during cathodic polarization. During anodic polarization, the current increased with increasing potential, indicating active anodic dissolution. Meanwhile, the anodic shape also demonstrates that there is a passive region of both the base alloy and the SiO_2-based alloys, which signifies that a protective surface film forms.

The electrochemical parameters derived from the polarization curves, including the corrosion potential (E_{corr}), the corrosion current density (I_{corr}), and the corrosion rate are highlighted in Tables 4. he findings reveal that the corrosion resistance of Ti-15Mo alloy was enhanced by the addition of SiO_2. In particular, the corrosion current density decreased from 8.619 μA/cm^2 for the base alloy to 7.8 μA/cm^2 at 0.5 wt% SiO_2 and further to 1.92 μA/cm^2 at 3 wt% SiO_2. This reduction in I_{corr} implies that the rate of corrosion decreases hence increased corrosion resistance.

Overall, it is possible to state that the improvement in corrosion performance can be may be associated with the role SiO_2 in promoting to the development of a more protective surface layer that reduces the rate of corrosion of the alloy under the simulated physiologic environment.

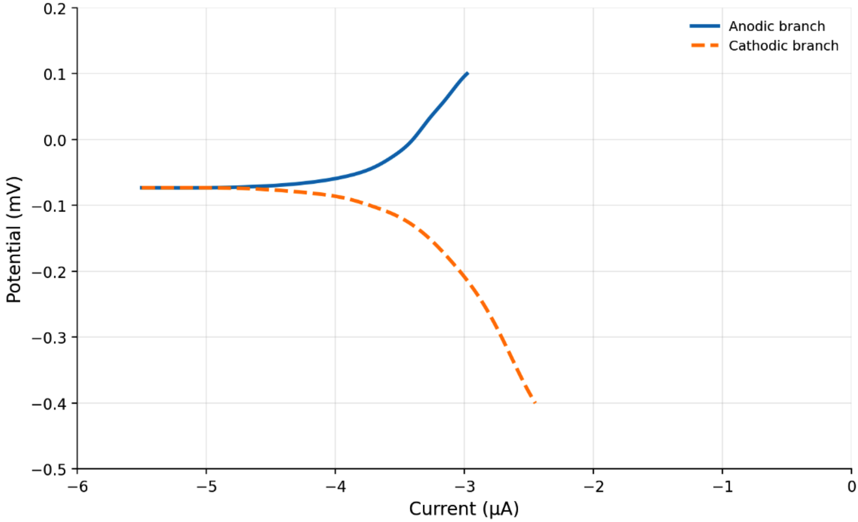

Fig. 3. **The corrosion potential Vs Current (μA) for (Ti15Mo) Base Alloy for Hank's solution**

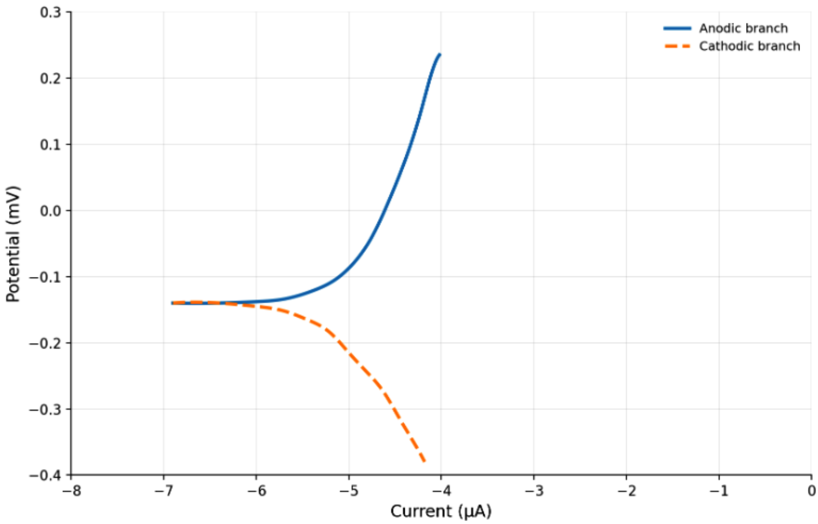

Fig. 4. **The corrosion potential Vs Current (μA) for (Ti15Mo-3%Sio_2) Alloy for Hank's solution**

Table 4. **Porosity, corrosion potential (E_{corr}), corrosion current density (I_{corr}), corrosion rate, and improvement percentage of all alloys in Hank's solution at 37±1°C**

wt%	Porosity (%)	Icorr. (μA/cm²)	Ecorr. (mv)	Corrosion rate (mpy)	Improvement (%)
0.0	18.24	8.619	–47	0.1411	
0.5	20.7	7.8	–58	0.1057	25.02
1.0	21.4	6.921	–136	5.49E-09	31.65
1.5	23.2	5.11	–197	0.0964	54.86
2.0	26.4	4.574	–50	0.0636	49.51
2.5	28.6	2.54	–102	0.0712	77.49
3.0	30.9	1.92	–70	0.0252	82.81

4. Conclusion

1. Silicon oxide addition enhanced the corrosion resistance of Ti-15Mo alloy. This became even better with increase in the SiO_2 content increased, reaching a maximum of 82.81% at 3 wt% SiO_2, when the corrosion rate declined to 0.0252 mpy.

2. The addition of SiO_2 to Ti-15Mo alloy improved the porosity of the specimen, with the largest porosity of 30.9%being observed at 3 wt% SiO_2. This change of composition was associated with better corrosion performance under the current experimental conditions.

3. Addition of SiO_2 to decrease the contact angle also was evident, with the highest decrement being observed at 3 wt. SiO_2. This result indicates improved surface wettability, which was correlated with the increased corrosion behavior of the alloy.

References:

1. de Viteri V. S., Fuentes E. Titanium and titanium alloys as biomaterials. Chap. 5 // Tribology — Fundamentals and Advancements / ed. by J. Gegner. — Rijeka: InTech, 2013. — P. 155–181.
2. El-Hajje A., Kolos E. C., Wang J. K., Maleksaeedi S., He Z., Wiria F. E. et al. Physical and mechanical characterization of 3D-printed porous titanium for biomedical applications // Journal of Materials Science: Materials in Medicine. — 2014. — Vol. 25, no. 11. — P. 2471–2480.
3. Al Deen H. H. J., Hamza S. J. Experimental study of the electrochemical and biological properties of (Nb-1%Zr — xGe) alloy for biomedical applications // NeuroQuantology. — 2022. — DOI: 10.14704/nq. 2022.

4. Haleem A. H., Radhi N. S., Jaber N. T., Al-Khafaji Z. Preparation and exploration of nano-multi-layers on 316L stainless steel for surgical tools // Jordan Journal of Mechanical and Industrial Engineering. — 2024. — Vol. 18, no. 2.
5. Hanawa T. Biocompatibility of titanium from the viewpoint of its surface // Science and Technology of Advanced Materials. — 2022. — Vol. 23, no. 1. — P. 457–472.
6. Hussein E. Y., Al-Murshdy J. M. S., Radhi N. S. Surface improvement of titanium alloys for biomedical applications by anodizing // Jordan Journal of Mechanical and Industrial Engineering. — 2024. — Vol. 18, no. 3.
7. Jung H.-D. Titanium and its alloys for biomedical applications // Metals. — 2021. — Vol. 11, no. 12. — Art. 1945.
8. Marin E., Lanzutti A. Biomedical applications of titanium alloys: a comprehensive review // Materials. — 2023. — Vol. 17, no. 1. — Art. 114.
9. Chakraborty R. et al. MWCNT reinforced bone-like calcium phosphate — hydroxyapatite composite coating developed through pulsed electrodeposition with varying amount of apatite phase and crystallinity to promote superior osteoconduction, cytocompatibility and corrosion protection performance compared to bare metallic implant surface // Surface and Coatings Technology. — 2017. — Vol. 325. — P. 496–514.
10. Li Y. et al. New developments of Ti-based alloys for biomedical applications // Materials. — 2014. — Vol. 7, no. 3. — P. 1709–1800.
11. Long M., Rack H. J. Titanium alloys in total joint replacement — a materials science perspective // Biomaterials. — 1998. — Vol. 19, no. 18. — P. 1621–1639.
12. Hanawa T. Recent development of new alloys for biomedical use // Materials Science Forum. — 2006. — Vol. 512.
13. Abdul-husien M., Al Deen H. H. J., Al-Roubai A. O. Improvement of corrosion and wear resistance of (Ti12Mo5Ta) alloy by germanium addition used in biomedical applications // Jordan Journal of Mechanical and Industrial Engineering. — 2024. — Vol. 7, no. 1.
14. More N. S. et al. Tribocorrosion behavior of β titanium alloys in physiological solutions containing synovial components // Materials Science and Engineering: C. — 2011. — Vol. 31, no. 2. — P. 400–408.
15. Geetha M. et al. Ti based biomaterials, the ultimate choice for orthopaedic implants — a review // Progress in Materials Science. — 2009. — Vol. 54, no. 3. — P. 397–425.

16. Niinomi M., Nakai M., Hieda J. Development of new metallic alloys for biomedical applications // Acta Biomaterialia. — 2012. — Vol. 8, no. 11. — P. 3888–3903.
17. Ikeda M., Ueda M., Niinomi M. Recent studies and developments in titanium biomaterials // MATEC Web of Conferences. — 2020. — Vol. 321.
18. ASTM. Standard practice for microetching metals and alloys. — United States of America: ASTM, 2005.
19. Şimşek I., Özyürek D. Investigation of wear and corrosion behaviors of Ti15Mo alloy produced by mechanical alloying method in SBF environment // Powder Metallurgy and Metal Ceramics. — 2019. — Vol. 58, no. 7. — P. 446–454.

МЕДИЦИНА И ФАРМАКОЛОГИЯ

Прогностические маркеры хронической болезни почек при метаболическом синдроме в разных возрастных группах

Тирабян Светлана Манвеловна, аспирант
Научный руководитель: Корнеева Елена Викторовна, кандидат медицинских наук, доцент;
Научный руководитель: Добрынина Ирина Юрьевна, доктор медицинских наук, профессор;
Научный руководитель: Арямкина Ольга Леонидовна, доктор медицинских наук, профессор
Сургутский государственный университет

Ожирение и сахарный диабет 2-го типа (СД2) являются ведущими причинами формирования хронической болезни почек (ХБП) в рамках кардиоренометаболического синдрома. Вопрос о вкладе различных фенотипов ожирения и возрастных особенностей в развитие ренальной дисфункции остается открытым. ***Цель исследования.*** *Изучить распространенность и структуру стадий ХБП у больных с метаболическим синдромом (МС) в различных возрастных группах.* ***Материалы и методы.*** *Проведен анализ 300 амбулаторных карт пациентов с МС (ожирение + СД2), разделенных на группы согласно возрастной номенклатуре Всемирной организации здравоохранения 2020 г.: молодые (n = 45), зрелые (n = 75) и пожилые (n = 180). Диагноз «хроническая болезнь почек» верифицирован по критериям KDIGO 2024 г. (скорость клубочковой фильтрации, альбуминурия, альбумин-креатининовое соотношение). Проведен частотный анализ с оценкой достоверности различий (критерий χ^2).* ***Результаты.*** *Распространенность ХБП увеличивалась с возрастом: у молодых — 22,2% (стадии С1–С2), у зрелых — 49,3% (стадии С2–С3а–С3b; p < 0,006), у пожилых — 57,7% (стадии С3а–С3b–С4; p < 0,001). Выявлено преобладание женщин (73,3%).* ***Выводы.*** *Возраст является ключевым фактором прогрессирования ХБП при МС. Частота ренальной дисфункции у лиц зрелого и пожилого возраста статисти-*

чески значимо выше, чем у молодых, что диктует необходимость раннего скрининга маркеров повреждения почек, начиная со зрелого возраста.

Ключевые слова: *хроническая болезнь почек, метаболический синдром, ожирение, сахарный диабет 2-го типа, кардиоренометаболический синдром, возрастные группы, скорость клубочковой фильтрации.*

Введение

Ожирение в современном мире представляет собой серьезную медико-социальную проблему. Доказано, что риски развития метаболического синдрома (МС) связаны не столько с общим объемом жировой массы, сколько с ее гормонально-метаболической активностью. Это послужило основанием для формирования концепции метаболического здоровья, которая легла в основу современной классификации ожирения. Наряду с сахарным диабетом 2-го типа (СД2), ожирение является основой для формирования МС, включающего коморбидность с артериальной гипертонией (АГ), ишемической болезнью сердца, дислипидемией и неалкогольной жировой болезнью печени [1, с. 45–50; 2].

СД2 и АГ признаны ведущими причинами развития хронической болезни почек (ХБП), что привело к формированию понятия «кардиоренометаболический синдром». Ожирение как базовый компонент МС также является значимым фактором риска развития ренальных дисфункций, однако единое мнение о вкладе его различных фенотипов в патогенез повреждения почек отсутствует [3]. В связи с высокой распространенностью ХБП при ожирении особую актуальность приобретает поиск ранних маркеров почечного повреждения, а также изучение их взаимосвязи с параметрами, характеризующими гормонально-метаболическую составляющую ожирения. Генетическая предрасположенность к развитию ожирения является перспективным направлением для персонифицированного ведения пациентов и оценки кардиометаболического риска [4].

Цель исследования — изучить распространенность и структуру стадий ХБП у больных с метаболическим синдромом в разных возрастных группах.

Материалы и методы

Работа выполнена по плану научно-исследовательской работы кафедры внутренних болезней БУ ВО ХМАО — Югры «Сургутский государственный университет» (№ АААА-А19–119062490051–6) на базе БУ ХМАО — Югры «Городская клиническая поликлиника № 1» за период 2025 год методом сплошной выборки.

Диагнозы (ожирение, СД2 и составляющие МС) устанавливались в соответствии с актуальными клиническими рекомендациями. Обследована когорта из 300 амбулаторных пациентов (220 женщин, 80 мужчин). Распределение по возрастным группам проводилось согласно номенклатуре Всемирной организации здравоохранения 2020 г.: молодые ($n = 45$), зрелые ($n = 75$) и пожилые ($n = 180$).

Оценка состояния почек проводилась согласно критериям KDIGO 2024 года. Всем пациентам выполнялся комплекс лабораторных исследований, включавший определение уровня альбуминурии, креатинина сыворотки крови с расчетом скорости клубочковой фильтрации (СКФ), альбумин-креатининового соотношения, показателей кальций-фосфатного метаболизма, а также индекса HOMA-IR и уровня мочевой кислоты (гиперурикемии).

Статистическая обработка данных проводилась с использованием методов частотного анализа. Для сравнения качественных показателей применяли критерий χ^2 Пирсона. Различия считались статистически значимыми при $p < 0{,}05$.

Результаты и обсуждение

Анализ гендерного состава исследуемой группы показал, что среди больных с ожирением и СД2 в рамках кардиоренометаболического синдрома в 2,75 раза преобладали женщины, что может быть связано как с гормональными особенностями, так и с более высокой обращаемостью женского населения за медицинской помощью.

При оценке функционального состояния почек были получены следующие результаты (таблица 1).

Таблица 1. **Распространенность и стадии ХБП в исследуемых группах**

Возрастная группа	**Выявлено ХБП, *n* (%)**	**Основные стадии ХБП**	χ^2	***p***
Молодые ($n = 45$)	10 (22,2%)	С1С2	—	—
Зрелые ($n = 75$)	37 (49,3%)	С2–С3а–С3b	7,58	<0,006
Пожилые ($n = 180$)	104 (57,7%)	С3а–С3b–С4	16,80	<0,001

В группе молодых пациентов дисфункция почек диагностирована у 10 человек (22,2%), при этом ХБП соответствовала начальным стадиям (С1–С2). У лиц зрелого возраста частота выявления ХБП была значимо выше, достигая 49,3% ($p < 0{,}006$), с преобладанием стадий С2–С3а–С3b, что свидетельствует о начале существенного снижения фильтрационной функции почек.

Наибольшая распространенность ХБП зафиксирована в группе пожилых пациентов — 104 случая (57,7%; $p < 0{,}001$). У данной категории больных диагностированы более тяжелые стадии заболевания — С3а–С3b–С4, что характеризует не только высокую частоту, но и глубину поражения почечной ткани.

Обращает на себя внимание частота встречаемости ХБП у лиц зрелого и пожилого возраста, которая оказалась сопоставимо высокой — 49,3 и 57,7% соответственно, что указывает на необходимость активного скрининга почечной дисфункции, начиная со зрелого возраста, когда процесс прогрессирования становится клинически значимым. Полученные данные коррелируют с результатами других исследователей, указывающих на кумулятивный эффект факторов риска (длительность ожирения, стаж СД2, артериальная гипертензия) в процессе старения организма [5].

Выводы

1. В исследуемой когорте больных с ожирением и СД2 в составе кардиоренометаболического синдрома отмечено значительное преобладание женщин (соотношение 2,75: 1).

2. ХБП диагностирована у половины обследованных пациентов (n = 151; 50,3%), при этом стадии поражения почек закономерно утяжелялись с возрастом: С1–С2 — у молодых; С2–С3a–С3b — у зрелых; С3a–С3b–С4 — у пожилых больных.

3. Снижение скорости клубочковой фильтрации и возрастание стадии ХБП прогрессируют по мере увеличения возраста пациентов. Высокая частота встречаемости ХБП у лиц зрелого возраста (49,3%) диктует необходимость раннего выявления маркеров почечного повреждения для своевременной нефропротективной терапии.

Литература:

1. Алгоритмы специализированной медицинской помощи больным сахарным диабетом. Вып. 10 / И. И. Дедов, М. В. Шестакова, А. Ю. Майоров [и др.]. — М.: [б. и.], 2023. — 230 с.
2. Консенсус по ведению пациентов с гиперурикемией и высоким сердечно-сосудистым риском: 2022 / И. Е. Чазова, Ю. В. Жернакова, О. А. Кисляк [и др.] // Системные гипертензии. — 2022. — Т. 19, № 1. — С. 5–22. — DOI: 10.38109/2075–082X-2022–1–5–22
3. Cardiovascular Complications in Chronic Kidney Disease: A Review from the European Renal and Cardiovascular Medicine Working Group of the European Renal Association / C. Zoccali, F. Mallamaci, M. Adamczak [et

al.] // Cardiovasc Res. — 2023. — Vol. 119, № 11. — P. 2017–2032. — DOI: 10.1093/cvr/cvad083

4. За пределами ИМТ: обсуждаем новую концепцию определения и диагностики клинического ожирения / Т. Ю. Демидова, О. А. Кисляк, А. В. Стародубова [и др.] // Медицинский совет. — 2025. — № 6. — С. 86–98. — DOI: 10.21518/ms2025–183
5. Федорова, Е. Ю. Ожирение и почки: механизмы повреждения почек при ожирении / Е. Ю. Федорова, Е. А. Краснова, М. В. Шестакова // Ожирение и метаболизм. — 2006. — № 1. — С. 22–28.

СЕЛЬСКОЕ ХОЗЯЙСТВО

Использование информационных технологий в сельском хозяйстве

Васильева Анжела Андреевна, студент
Научный руководитель: Арасланбаев Ирек Вакильевич, кандидат экономических наук, доцент
Башкирский государственный аграрный университет (г. Уфа)

В работе рассматриваются современные информационные технологии, применяемые в сельском хозяйстве, их влияние на эффективность аграрного производства и экономическую отдачу. Анализируются ключевые решения (точное земледелие, IoT, Big Data), приводятся примеры внедрения в России и за рубежом, оцениваются экономические выгоды и барьеры внедрения. Делаются выводы о перспективах цифровизации отрасли.

Ключевые слова: *информационные технологии, сельское хозяйство, агросектор, искусственный интеллект, автоматизация.*

Современное сельское хозяйство переживает этап глубокой технологической трансформации. Внедрение информационных технологий (ИТ) становится не просто трендом, а необходимым условием повышения конкурентоспособности аграрного сектора. Рост населения, ограниченность природных ресурсов, изменение климата и требования к экологической устойчивости вынуждают отрасль искать новые подходы к управлению производством.

Информационные технологии в сельском хозяйстве охватывают широкий спектр решений — от спутникового мониторинга до искусственного интеллекта. Их внедрение позволяет перейти от интуитивных решений к научно обоснованному управлению агропроизводством.

Концепция точного земледелия (Precision Agriculture) основана на дифференцированном управлении агрооперациями с учётом неоднородности полей [4]. В её основе лежит принцип, что разные участки одного поля могут требовать разного количества удобрений, воды или семян. Для реализации этого подхода используются GPS/ГЛОНАСС-навигация для точного позиционирования техники, датчики влажности, температуры и плодородия почвы, а также дроны и спутники для аэрофотосъёмки и построения карт вегетации (NDVI). Экономический эффект достигается за счёт сокращения затрат на удобрения и средства защиты растений на 15–30%, повышения урожайности на 10–20% и снижения экологического ущерба от перерасхода химикатов. Например, точечное внесение удобрений только на те участки поля, где это действительно необходимо, позволяет не только сэкономить средства, но и уменьшить загрязнение грунтовых вод.

Интернет вещей (IoT) и датчики играют всё более значимую роль в современном сельском хозяйстве [4]. Датчики, установленные в полях, теплицах или на фермах, передают данные в режиме реального времени, что позволяет оперативно реагировать на изменения условий. В теплицах датчики микроклимата контролируют температуру, влажность, уровень освещённости и концентрацию углекислого газа, автоматически регулируя системы отопления, вентиляции и орошения. На животноводческих фермах носимые датчики отслеживают активность, температуру тела и частоту дыхания животных, что помогает своевременно выявлять заболевания и предотвращать их распространение [5]. В растениеводстве датчики микроклимата в сочетании с моделями прогнозирования позволяют предсказать вспышки болезней растений и принять превентивные меры. Внедрение IoT сокращает потери урожая на 5–15% и снижает затраты на ветеринарное обслуживание.

Искусственный интеллект (ИИ) и машинное обучение всё активнее внедряются в сельскохозяйственные процессы [3]. Алгоритмы компьютерного зрения, установленные на дронах или наземной технике, способны распознавать сорняки среди культурных растений и точечно распылять гербициды только на проблемные участки. Это не только экономит средства, но и снижает химическую нагрузку на окружающую среду. В сортировке продукции ИИ-системы автоматически классифицируют фрукты и овощи по размеру, цвету и наличию дефектов, отбраковывая некачественные экземпляры. В животноводстве ИИ анализирует поведение животных, выявляя отклонения от нормы, которые могут свидетельствовать о начале заболевания. Прогнозирование цен на сельхозпродукцию с помощью ИИ помогает фермерам выбирать оптимальное время для продажи, максимизируя прибыль.

Роботизация и автоматизация снижают трудозатраты и риски человеческого фактора [4]. Роботы для прополки, сбора урожая или доения коров работают круглосуточно, не устают и не допускают ошибок из-за невнимательности. Например, роботы Lely, используемые на молочных фермах в Нидерландах, автоматизируют процесс доения, повышая надои на 5–8% за счёт регулярного и комфортного доения в соответствии с потребностями каждой коровы. Автономные тракторы и комбайны, оснащённые системами ИИ и GPS, выполняют посев, обработку и уборку с высокой точностью, минимизируя перекрытия и пропуски. В теплицах роботы собирают ягоды или овощи, распознавая степень их зрелости с помощью камер и алгоритмов машинного зрения.

Цифровые двойники полей и ферм — ещё одно перспективное направление [3]. Виртуальная модель хозяйства, синхронизированная с реальными данными с датчиков и дронов, позволяет моделировать различные сценарии управления: как изменится урожайность при изменении норм внесения удобрений, какой будет эффект от внедрения нового сорта или как повлияет на продуктивность изменение графика полива. Это даёт возможность тестировать управленческие решения без риска для реального производства.

Блокчейн-технологии находят применение в отслеживании цепочки поставок сельхозпродукции [3]. Прозрачная и неизменяемая запись о происхождении товара, условиях его производства и транспортировки повышает доверие потребителей и позволяет премировать производителей, соблюдающих высокие стандарты качества и экологичности. Например, покупатель может отсканировать QR-код на упаковке мяса и увидеть всю историю его производства: от фермы, где выращивался скот, до даты и времени убоя и условий транспортировки.

Облачные платформы объединяют все эти технологии в единую экосистему [2]. Фермер получает доступ к данным с датчиков, дронов и метеостанций через веб-интерфейс или мобильное приложение. Платформа автоматически анализирует информацию и выдаёт рекомендации: когда и сколько поливать, какие удобрения вносить, когда начинать уборку [2]. Некоторые системы даже интегрируются с бухгалтерской программой, позволяя оценить экономическую эффективность каждого агроприёма.

Примеры внедрения ИТ в сельском хозяйстве демонстрируют их реальную пользу. В России агрохолдинги «Мираторг», «Черкизово» и «Русагро» внедряют системы точного земледелия и IoT [1]. По данным Минсельхоза РФ, цифровизация позволила снизить себестоимость зерна на 7–12% в пилотных хозяйствах за счёт оптимизации расхода топлива, семян и удобрений [1]. В США компания John Deere оснащает свою технику ИИ-системами для автоматического управления посевом и уборкой. Это сократило время простоя техники на 20% и повысило точность выполнения операций. В Нидерландах вертикальные фермы с ИИ-управлением микроклиматом дают урожай в 10 раз выше с единицы площади, чем традиционные теплицы, при этом потребляя на 90% меньше воды.

Экономические эффекты от цифровизации проявляются в нескольких ключевых показателях. Во-первых, снижается себестоимость продукции на 10–25% за счёт оптимизации ресурсов: топлива, удобрений, воды, рабочей силы [4]. Во-вторых, растёт урожайность или продуктивность на 10–30% благодаря точному управлению агроприёмами [4]. В-третьих, сокращается срок окупаемости инвестиций в ИТ до 2–4 лет в крупных хозяйствах [4]. В-четвёртых, уменьшается экологический след: снижается выброс $CO2$ от сельхозтехники, экономится вода, уменьшается загрязнение почв и водоёмов химикатами.

Однако распространение ИТ в сельском хозяйстве сдерживается рядом барьеров. Высокая стоимость оборудования — дронов, датчиков, программного обеспечения — делает его недоступным для малых фермерских хозяйств [4]. Нехватка квалифицированных кадров, способных работать с новыми технологиями, также тормозит внедрение [4]. Слабая инфраструктура в сельской местности — отсутствие стабильного интернета, перебои с энергоснабжением — ограничивает возможности использования облачных платформ и IoT [4]. Консерватизм аграриев, привыкших к традиционным методам работы, и недостаточная господдержка в ряде регионов дополнительно усложняют процесс цифровизации.

В России госпрограмма «Цифровое сельское хозяйство» предусматривает ряд мер для ускорения внедрения ИТ [1]. Среди них — субсидии на покупку ИТ-решений, создание единой цифровой платформы для агросектора, объединяющей данные о погоде, почве, рынках и господдержке, а также обучение фермеров работе с новыми технологиями. К 2030 году ожидается, что до 50% сельхозпредприятий в развитых странах перейдут на модели точного земледелия [1]. ИИ станет стандартом управления агробизнесом.

Использование информационных технологий трансформирует сельское хозяйство из традиционно ресурсоёмкой отрасли в высокотехнологичный сектор экономики. Внедрение точного земледелия, IoT, Big Data и ИИ позволяет существенно повысить экономическую эффективность, снизить экологическую нагрузку и адаптироваться к глобальным вызовам.

Литература:

1. Государственная программа «Цифровое сельское хозяйство»: утв. Минсельхозом РФ. — Москва, 2023. — 45 с.

2. Агросигнал: платформа управления агропроизводством: официальный сайт. — URL: https://agrosignal.com/ (дата обращения: 15.04.2024). — Текст: электронный.
3. Ганеева А. М., Арасланбаев И. В. Роль информатизации в современном обществе // Актуальные вопросы экономико-статистического исследования и информационных технологий: сборник научных статей: посвящается 40-летию создания кафедры «Статистики и информационных систем в экономике» / МСХ РФ, Башкирский государственный аграрный университет. — Уфа, 2011. — С. 275–276.
4. Топоркова С. И., Арасланбаев И. В. Перспективы использования информационных технологий в сельской местности // Актуальные вопросы экономико-статистического исследования и информационных технологий: сборник научных статей: посвящается 40-летию создания кафедры «Статистики и информационных систем в экономике» /МСХ РФ, Башкирский государственный аграрный университет. — Уфа, 2011. — С. 267–268.
5. Фатеева Т. Н., Лукьянченко М. С. Цифровизация агропромышленного комплекса России: опыт и перспективы развития / Т. Н. Фатеева // Вестник Алтайской академии экономики и права. — 2023. — № 2. — С. 123–129.
6. Цифровая трансформация агропромышленного комплекса / Т. И. Ашмарина, Т. В. Бирюкова, В. Т. Водянников [и др.]. — Москва: Общество с ограниченной ответственностью «Мегаполис», 2022. — 160 с. — ISBN 978–5–6049097–8–2.
7. Экономическая эффективность цифровых технологий в животноводстве // Научная электронная библиотека КиберЛенинка / А. В. Иванов, С. П. Петрова. — 2023. — URL: https://cyberleninka.ru/article/n/ekonomicheskaya-effektivnost-tsifrovyh-tehnologiy-v-zhivotnovodstve (дата обращения: 16.04.2026). — Текст: электронный.

МЕНЕДЖМЕНТ

Female Entrepreneurship and Work-Life Balance: Opportunities, Challenges, and Support Systems

Kuandykova Sholpan, Lecturer
SDU University (Kaskelen, Kazakhstan)

This paper examines the relationship between female entrepreneurship and work-life balance, with a focus on structural barriers, digital opportunities, and socio-cultural influences. Drawing on entrepreneurship theories and gender inequality frameworks, the study explores how women navigate business and personal responsibilities. The findings suggest that while entrepreneurship offers flexibility, it also intensifies time-related pressures due to unpaid care work and limited institutional support. The role of digital platforms in enabling flexible work is highlighted, alongside cultural expectations that shape women's entrepreneurial experiences. The paper concludes with practical implications for policymakers, educators, and business support organizations, with specific reference to Kazakhstan.

Keywords: *entrepreneurship, female entrepreneurship, challenges and opportunities*

Introduction

Female entrepreneurship has grown steadily over the last two decades, but balancing business demands with family and personal responsibilities remains one of the most persistent challenges. Recent global evidence shows that women's startup activity has increased, yet the gender gap in entrepreneurship still exists in many countries. The GEM 2023/24 Women's Entrepreneurship Report found that women's startup activity rose from an average of 6.1% in 2001–2005 to 10.4% in 2021–2023 across 30 countries, while the OECD estimates that women remain underrepresented among active entrepreneurs and face structural barriers such as limited access to finance and networks.

This article argues that work-life balance is not a private problem of individual women entrepreneurs alone. It is shaped by family support, childcare systems, social expectations, financial resources, and the wider economic context. Research shows that women's entrepreneurial success is closely linked to these conditions, especially where care responsibilities and business demands overlap.

Literature Review

Female entrepreneurship has attracted increasing scholarly attention over the past two decades, particularly in relation to work-life balance, gender inequality, and access to resources. Existing literature highlights that while entrepreneurship offers women flexibility and autonomy, it also creates new forms of pressure due to overlapping professional and domestic responsibilities.

A foundational contribution by Agarwal and Lenka (2015) identifies work-life balance as a central theme in research on women entrepreneurs. Their review argues that women are more likely than men to experience role conflict because they simultaneously manage business responsibilities and traditional family roles. The authors emphasize that entrepreneurship is often perceived as a solution to rigid employment structures; however, it can intensify workload and blur the boundaries between personal and professional life.

Empirical studies support this perspective by demonstrating that women entrepreneurs frequently operate under conditions of «double burden,» where paid work and unpaid care responsibilities coexist. Edralin (2012) found that women entrepreneurs adopt various coping strategies, such as integrating business activities into home environments and practicing time management techniques. While these strategies provide flexibility, they may also reinforce the merging of work and family domains, making it difficult to achieve true balance.

Cross-national research further highlights that work-life balance is not a universal experience but is shaped by economic and institutional contexts. Kaciak and Welsh (2020) analyzed women entrepreneurs across multiple countries and found that levels of work-family conflict and family support vary depending on national development and cultural norms. Their findings suggest that women in middle-income economies may experience higher levels of tension due to limited institutional support combined with increasing economic participation.

Recent literature has shifted focus toward the role of support systems in improving entrepreneurial outcomes. Yang et al. (2025) conducted a systematic review and concluded that family support plays a critical role in enhancing women's well-being and business sustainability. Importantly, the study identifies work-life balance as a mediating factor between support systems and entrepreneurial success, indicating that the presence of support alone is insufficient without effective balance mechanisms.

In addition to family-level factors, structural barriers continue to shape women's entrepreneurial experiences. Reports by the Organisation for Economic Co-operation and Development (OECD, 2025) show that women face persistent challenges in accessing finance, business networks, and training opportunities. Women are less likely to secure external funding and tend to rely on personal savings, which limits business growth potential.

The unequal distribution of unpaid care work remains one of the most significant constraints. According to the World Bank (2026), women globally spend significantly more time on caregiving activities than men, reducing their ability to fully engage in entrepreneurial activities. The report highlights that lack of affordable childcare services directly impacts women's capacity to start and scale businesses, reinforcing gender disparities in entrepreneurship.

At the same time, digital transformation has created new opportunities for women entrepreneurs. Online platforms allow women to enter markets with lower financial barriers and greater flexibility. However, the literature also warns that digital entrepreneurship can extend working hours and increase expectations for constant availability, thereby complicating work-life balance rather than resolving it.

Overall, the literature suggests that female entrepreneurship exists at the intersection of opportunity and constraint. While entrepreneurship can empower women economically, its success and sustainability depend heavily on social support systems, institutional frameworks, and the ability to manage competing life roles. This reinforces the need to view work-life balance not merely as an individual responsibility but as a broader socio-economic issue.

Theoretical Framework

Understanding female entrepreneurship and work-life balance requires integrating insights from both entrepreneurship theory and gender studies. This section outlines the key theoretical perspectives that explain why women enter entrepreneurship and why their experiences differ from men's.

Entrepreneurship Theories

Opportunity-Based vs. Necessity-Based Entrepreneurship

Entrepreneurship is commonly divided into opportunity-driven and necessity-driven forms. Opportunity-based entrepreneurship occurs when individuals identify and exploit a market gap, often motivated by independence, innovation, or profit. In contrast, necessity-based entrepreneurship arises when individuals lack alternative employment options.

For many women, entrepreneurship lies at the intersection of these two categories. On the one hand, digitalization and flexible work opportunities allow women to identify and pursue business ideas. On the other hand, rigid labor markets and limited work flexibility push women — especially mothers — toward self-employment as a practical solution. This dual motivation helps explain why women may enter entrepreneurship but still face structural constraints.

Resource-Based View (RBV)

The resource-based view suggests that business success depends on access to valuable resources, including financial capital, education, skills, and social networks. From this perspective, women's entrepreneurial outcomes are shaped by unequal access to these resources.

Research consistently shows that women:

— have less access to external financing
— rely more on personal or family funds
— have smaller professional networks

These limitations affect not only business growth but also the ability to outsource tasks or invest in support systems, which directly impacts work-life balance.

Human and Social Capital Theory

Human capital (education, skills, experience) and social capital (networks, relationships) are critical for entrepreneurship. While women's educational attainment has improved globally, gaps remain in access to business training and mentorship.

Social capital is particularly important for women entrepreneurs, as strong networks can provide:

— emotional support
— business advice
— access to markets and funding

However, women often have less access to influential business networks, which can limit their opportunities.

Gender Inequality Frameworks

Social Role Theory

Social role theory explains that men and women are expected to fulfill different roles in society. Women are typically associated with caregiving and domestic responsibilities, while men are associated with professional and leadership roles.

These expectations influence:

— how women allocate their time
— how society perceives women entrepreneurs
— how women evaluate their own success

As a result, women may prioritize family responsibilities even when running a business, creating tension between roles.

Institutional Theory

Institutional theory focuses on how formal (laws, policies) and informal (norms, culture) institutions shape behavior. In the context of female entrepreneurship, institutions determine access to:

— childcare services
— financial support programs
— legal protections

Weak institutional support can increase the burden on women, forcing them to rely on informal solutions such as family support.

Gendered Division of Labor

This framework highlights the unequal distribution of unpaid work. Women perform a disproportionate share of household and caregiving tasks, which reduces the time and energy available for business activities.

This «double burden» is one of the main reasons why work-life balance is more difficult for women entrepreneurs than for men.

Main Discussion

Barriers Faced by Women Entrepreneurs

Women entrepreneurs face a combination of structural, economic, and social barriers that directly affect both business performance and personal well-being.

One of the most significant barriers is time constraint. Women are more likely to be responsible for childcare and household duties, which limits the time they can dedicate to business activities. This often leads to fragmented working hours and reduced productivity.

Another major challenge is limited access to finance. Women are less likely to receive bank loans or investment funding and often start businesses with smaller amounts of capital. This restricts their ability to scale operations, hire employees, or invest in technology.

In addition, gender bias and stereotypes continue to influence how women entrepreneurs are perceived. Women may be seen as less competent or less committed to business, especially if they have family responsibilities. These biases can affect access to opportunities, partnerships, and funding.

Finally, women entrepreneurs often experience higher levels of stress and burnout. The constant need to balance multiple roles — business owner, caregiver, and household manager — creates emotional and psychological pressure.

In Kazakhstan, these challenges are particularly visible among small business owners, where women frequently manage both entrepreneurial activities and family responsibilities without formal support systems.

Role of Digital Platforms

Digital platforms such as Instagram, TikTok, and LinkedIn have transformed the landscape of female entrepreneurship.

These platforms offer several advantages:

— Low entry barriers: Women can start businesses without significant initial investment

— Flexibility: Work can be done from home and at convenient times

— Direct access to customers: No need for physical stores or intermediaries

— Personal branding opportunities

In Kazakhstan, many women use Instagram to run small businesses such as clothing shops, beauty services, and food delivery. This model allows them to combine entrepreneurship with family responsibilities.

However, digital entrepreneurship also introduces new challenges. The expectation of constant online presence can blur the boundaries between work and personal life. Women may feel pressure to respond to customers at all times, leading to extended working hours and reduced rest.

Thus, while digital platforms create opportunities, they do not automatically solve work-life balance issues.

Cultural and Social Factors

Cultural and social norms play a crucial role in shaping women's entrepreneurial experiences.

In many societies, including Kazakhstan, traditional expectations position women as primary caregivers. These expectations can:

— limit women's time for business

— influence family support levels

— shape women's own priorities

Family support is a key factor. Women who receive help from partners or extended family are more likely to succeed and maintain balance. In contrast, lack of support can significantly increase stress and reduce business performance.

At the same time, social attitudes are gradually changing. In urban areas such as Almaty, female entrepreneurship is becoming more accepted, and women are increasingly encouraged to pursue professional and business goals.

Additionally, the growth of female networks and communities provides new forms of support. These networks offer mentorship, collaboration opportunities, and emotional encouragement, helping women overcome challenges.

Interconnection of Factors

It is important to note that these factors do not operate independently. Instead, they interact in complex ways:

— Limited finance can increase workload, affecting work-life balance
— Cultural expectations can reduce access to networks and opportunities
— Digital tools can both support and complicate balance

This interconnected nature highlights that female entrepreneurship is a multidimensional issue requiring integrated solutions.

Theoretical and Analytical Implications

The findings of this study reinforce the idea that female entrepreneurship should not be viewed solely as an economic activity but as a multi-dimensional phenomenon shaped by social, cultural, and institutional factors. The interaction between entrepreneurship theories and gender inequality frameworks demonstrates that women's entrepreneurial experiences are structurally different from those of men.

In particular, the analysis highlights that work-life balance functions as a mediating factor between access to resources and entrepreneurial outcomes. Even when women have business opportunities or skills, their ability to succeed is constrained by time limitations, unpaid care responsibilities, and social expectations. This suggests that traditional entrepreneurship theories, which often assume equal access to resources and time, may not fully capture the realities of female entrepreneurs.

Furthermore, the study contributes to the growing body of literature that emphasizes the importance of contextual factors, especially in emerging economies such as Kazakhstan. Cultural norms, institutional support systems, and levels of digital development significantly influence how women experience entrepreneurship and balance competing roles.

Practical Implications for Stakeholders

Policymakers

For policymakers, the findings suggest that promoting female entrepreneurship requires more than financial support. While access to funding remains important, social infrastructure plays an equally critical role.

Governments should:

— Invest in affordable and accessible childcare services, particularly in urban and semi-urban areas
— Develop targeted financial programs, such as microloans and grants specifically for women entrepreneurs

— Support flexible work policies and legal frameworks that enable women to combine business and family responsibilities

— Encourage the formalization of small businesses, especially those operating through digital platforms

In Kazakhstan, strengthening these areas could significantly improve both participation and sustainability of women-led businesses.

Educational Institutions

Educational institutions have a key role in preparing future women entrepreneurs. The analysis shows that skills development alone is not sufficient unless it is aligned with real-life challenges.

Universities and training centers should:

— Integrate entrepreneurship education with practical skills, such as digital marketing, financial literacy, and time management

— Include modules on work-life balance strategies and stress management

— Provide mentorship programs, connecting students with successful female entrepreneurs

— Encourage female participation in business-related fields

This approach can help women build not only knowledge but also confidence and resilience.

Business Support Organizations and Ecosystems

Organizations that support entrepreneurship (incubators, accelerators, NGOs) can play a crucial role in reducing gender-based barriers.

They should:

— Create women-focused business networks to increase access to social capital

— Offer flexible training formats (online, part-time) to accommodate women's schedules

— Provide psychological and peer support, recognizing the emotional challenges of entrepreneurship

— Facilitate access to funding opportunities and investors

Developing inclusive entrepreneurial ecosystems can significantly improve business outcomes for women.

Women Entrepreneurs

At the individual level, women entrepreneurs can benefit from adopting specific strategies to improve work-life balance.

These include:

— Setting clear boundaries between work and personal time

— Using digital tools efficiently rather than being constantly available
— Delegating tasks where possible (both in business and at home)
— Building support networks, including family, friends, and professional communities
— Prioritizing mental health and well-being

Importantly, women should avoid the unrealistic expectation of «doing everything perfectly» and instead focus on sustainable approaches to both work and life.

Key Recommendations

Based on the analysis, several key recommendations emerge:

1. Strengthen childcare infrastructure to reduce the unpaid care burden
2. Improve access to finance through targeted programs for women
3. Promote digital entrepreneurship while addressing its risks (e. g., burnout)
4. Encourage cultural change toward more equal distribution of household responsibilities
5. Develop integrated support systems, combining financial, educational, and social support

These recommendations highlight that improving work-life balance is not only an individual responsibility but a shared societal and institutional task.

Final Insight

Ultimately, the concept of «having it all» should be reconsidered. Rather than expecting women to perfectly balance all roles, the focus should shift toward creating realistic, supportive environments where women can succeed without excessive pressure.

Conclusion

Female entrepreneurship is not only about starting a business. It is also about sustaining a business while managing family life, personal well-being, and social expectations. The literature shows that work-life balance improves when women have access to family support, childcare, flexible work arrangements, mental health support, and fairer institutional policies. It also shows that entrepreneurship policy should move beyond encouraging women to «work harder» and instead build conditions that make balanced growth possible.

In the end, women can build successful businesses and maintain meaningful personal lives, but this is much more achievable when support systems are strong. Work-life balance is therefore not just an individual skill; it is a shared responsibility of families, employers, communities, and policymakers.

References:

1. Agarwal, S., & Lenka, U. (2015). Study on work-life balance of women entrepreneurs — review and research agenda. Industrial and Commercial Training, 47 (7), 356–362.
2. Edralin, D. M. (2012). Innovative Work-Life Balance Strategies of Filipina Entrepreneurs: New Evidence from Survey and Case Research Approaches. Procedia — Social and Behavioral Sciences.
3. GEM Consortium. (2024). GEM 2023/24 Women's Entrepreneurship Report: Reshaping Economies and Communities.
4. Global Entrepreneurship Monitor (GEM). (2024). Women's entrepreneurship report 2023/24
5. Kaciak, E., & Welsh, D. H. B. (2020). Women entrepreneurs and work — life interface: The impact of sustainable economies on success. Journal of Business Research, 112, 281–290.
6. OECD. (2025). Bridging the Finance Gap for Women Entrepreneurs.
7. Organisation for Economic Co-operation and Development (OECD). (2025). Bridging the finance gap for women entrepreneurs.
8. Sharma, S., & Upadhyay, P. S. (2025). Impact of Work-Life Balance Policies and Practices on Work Engagement of Women Entrepreneurs. Journal of Information Systems Engineering and Management.
9. Yang, S., Tran, M. H., & Wiklund, J. (2025). Family support, work-life balance and entrepreneurial well-being: a global systematic review with a gendered perspective. International Journal of Entrepreneurial Behavior & Research.
10. World Bank. (2026). Unlocking Women's Entrepreneurship through Childcare Reform.

Научное издание

Исследования молодых ученых

Выпускающий редактор Г. А. Письменная
Ответственные редакторы Е. И. Осянина, О. А. Шульга, З. А. Огурцова
Подготовка оригинал-макета О. В. Майер

Материалы публикуются в авторской редакции.

Подписано в печать 28.04.2026. Формат 60х84/16. Усл. печ. л. 4,0.
Тираж 300 экз.

Издательство «Молодой ученый».
420029, Республика Татарстан, г. Казань, ул. Академика Кирпичникова, д. 25.

Отпечатано в типографии издательства «Молодой ученый»,
Республика Татарстан, г. Казань, ул. Академика Кирпичникова, д. 25.